Opposing roles of E3 ligases TRIM23 and TRIM21 in regulation of ion channel ANO1 protein levels

Received for publication, August 19, 2020, and in revised form, April 19, 2021 Published, Papers in Press, May 3, 2021,
https://doi.org/10.1016/j.jbc.2021.100738

Xu Cao[1,‡], Zijing Zhou[1,‡], Ye Tian[1], Zhengzhao Liu[1,2,3], Kar On Cheng[1], Xibing Chen[1], Wenbao Hu[1], Yuk Ming Wong[1], Xiaofen Li[1], Hailin Zhang[4], Ronggui Hu[2,5,6], and Pingbo Huang[1,7,8,9,10,*]

From the [1]Division of Life Science, Hong Kong University of Science and Technology, Hong Kong, People's Republic of China; [2]State Key Laboratory of Molecular Biology, Shanghai Institute of Biochemistry and Cell Biology, Center for Excellence in Molecular Cell Science, Chinese Academy of Sciences, Shanghai, China; [3]Xiangya Hospital, Central South University, Changsha, China; [4]Department of Pharmacology, Hebei Medical University, Shijiazhuang, People's Republic of China; [5]Cancer Center, Shanghai Tenth People's Hospital, School of Medicine, Tongji University, Shanghai, China; [6]School of Life Science, Hangzhou Institute for Advance Study, University of Chinese Academy of Sciences, Hangzhou, China; [7]Department of Chemical and Biological Engineering, [8]State Key Laboratory of Molecular Neuroscience, [9]HKUST Shenzhen Research Institute, [10]Hong Kong Branch of Guangdong Southern Marine Science and Engineering Laboratory (Guangzhou), Hong Kong University of Science and Technology, Hong Kong, People's Republic of China

Edited by Mike Shipston

Anoctamin-1 (ANO1) (TMEM16A) is a calcium-activated chloride channel that plays critical roles in diverse physiological processes, such as sensory transduction and epithelial secretion. ANO1 levels have been shown to be altered under physiological and pathological conditions, although the molecular mechanisms that control ANO1 protein levels remain unclear. The ubiquitin–proteasome system is known to regulate the levels of numerous ion channels, but little information is available regarding whether and how ubiquitination regulates levels of ANO1. Here, we showed that two E3 ligases, TRIM23 and TRIM21, physically interact with the C terminus of ANO1. *In vitro* and *in vivo* assays demonstrated that whereas TRIM23 ubiquitinated ANO1 leading to its stabilization, TRIM21 ubiquitinated ANO1 and induced its degradation. Notably, ANO1 regulation by TRIM23 and TRIM21 is involved in chemical-induced pain sensation, salivary secretion, and heart-rate control in mice, and TRIM23 also mediates ANO1 upregulation induced by epidermal growth factor treatment. Our results suggest that these two antagonistic E3 ligases act together to control ANO1 expression and function. Our findings reveal a previously unrecognized mechanism for regulating ANO1 protein levels and identify a potential molecular link between ANO1 regulation, epidermal growth factor, and other signaling pathways.

Anoctamin-1 (ANO1; also called transmembrane protein 16A) is a calcium-activated chloride channel that plays key roles in epithelial secretion, sensory transduction, smooth and skeletal muscle contraction, cell proliferation and migration, and fertilization (1, 2). Recent cryo-EM structural studies have revealed that ANO1 features ten transmembrane domains and cytosolic N and C termini (3). Alternative splicing and the use of alternative initiation sites generate various ANO1 isoforms in which four segments, called a, b, c, and d, are skipped or included, and these isoforms exhibit distinct functional properties (4).

The function of plasmalemmal ion channels such as ANO1 is regulated through the alteration of either single-channel gating or cell-surface protein expression, and ANO1 protein levels are known to vary under distinct physiological and pathological conditions. For instance, long-term interleukin-4 stimulation of airway epithelia increases Ca^{2+}-activated chloride secretion at least partially by upregulating the ANO1 mRNA level (4), and chronic epidermal growth factor (EGF) treatment of epithelial cells upregulates ANO1 protein and mRNA levels (5). Notably, ANO1 overexpression is associated with numerous cancers, including head and neck squamous cell carcinoma (HNSCC), breast cancer, gastrointestinal stromal tumors, and prostate carcinoma (6–9), and aberrant ANO1 protein levels are also implicated in other diseases such as asthma (10), cerebrovascular remodeling during hypertension (11), diabetic gastroparesis, and airway goblet-cell metaplasia (7, 12). However, the molecular mechanisms through which ANO1 protein levels are altered under these physiological and pathological conditions remain unclear. Ubiquitination is recognized as a key mechanism that controls ion channel expression, particularly channel insertion into and retrieval from the cell surface, but little is known regarding whether and how ANO1 is regulated by the ubiquitin system under specific physiological or pathological conditions.

The E3 ubiquitin ligases TRIM21 (Ro52 or Ro/SSA) and TRIM23 (ARD1) belong to the tripartite motif (TRIM)-containing protein superfamily, one of the largest gene families (>70 members) in humans and mice. The TRIM at the N terminus of TRIM-family proteins includes a RING finger domain, 1 or 2 B-box zinc-finger domains, and a coiled-coil domain (13); conversely, at the C-terminal end, these proteins contain domains that perform distinct functions, with

‡ These authors contributed equally to the work.
* For correspondence: Pingbo Huang, bohuangp@ust.hk.

TRIM21 and TRIM23 harboring a PRY/SPRY domain and an ADP-ribosylation factor (ARF) domain, respectively. Both TRIM21 and TRIM23 have been localized in the cytoplasm and the nucleus (14). Although the RING domain of all TRIM proteins can potentially exhibit E3 ligase activity, the ligase activity has been experimentally validated only in the case of some of the proteins, including TRIM21 and TRIM23 (13, 15). Moreover, the E3 ligase activity of TRIM proteins participates in various physiological and pathological processes, including development, apoptosis, innate immunity, heart disease, and cancer.

Here, we report that both TRIM23 and TRIM21 physically interact with ANO1, and, more importantly, that TRIM23 ubiquitinates and thereby stabilizes ANO1, whereas TRIM21 ubiquitinates and causes ANO1 degradation. Our study thus reveals that two antagonistic E3 ligases function together to control ANO1 channel expression and physiological functions.

Results

ANO1 physically interacts with TRIM23

To investigate whether the ubiquitin system regulates ANO1, we performed yeast two-hybrid screening to identify potential E3 ubiquitin ligases of ANO1. Screening of our homemade E3 ligase library (16) with ANO1 C terminus (ANO1C) as the bait identified TRIM23 E3 ligase as a binding partner (Fig. 1*A*).

Physical interaction between ANO1 and TRIM23 was further substantiated through pull-down and coimmunoprecipitation (co-IP) assays performed using HEK293T cells expressing epitope-tagged ANO1 and TRIM23: glutathione-*S*-transferase (GST)-ANO1C but not GST alone pulled down hemagglutinin (HA)-tagged TRIM23 (HA-TRIM23) (Fig. 1*B*), and V5-tagged full-length ANO1 (ANO1–V5) coprecipitated with both HA-TRIM23 and RING-domain–deleted HA-TRIM23 (HA-TRIM23ΔRING) (Fig. 1*C*). Moreover, in co-IPs performed using human ZR-75-1 cells, anti-TRIM23 but not control immunoglobulin G coprecipitated endogenous ANO1 and TRIM23 (Fig. 1*D*), which confirmed that the endogenous proteins also interact with each other. ZR-75-1 cells were selected as the cell model because ANO1 is abundantly expressed in these cells (6). Here, ANO1 was recognized by a validated anti-human–ANO1 antibody (ab64085, Abcam) (Fig. S1*A*) as the only major band (~160 kDa) in ZR-75-1 cells (Fig. S2*A*); the protein size agreed with that reported previously in a study that confirmed ANO1 identity in Western blotting by using siRNA techniques (6) (M. Bentires-Alj,

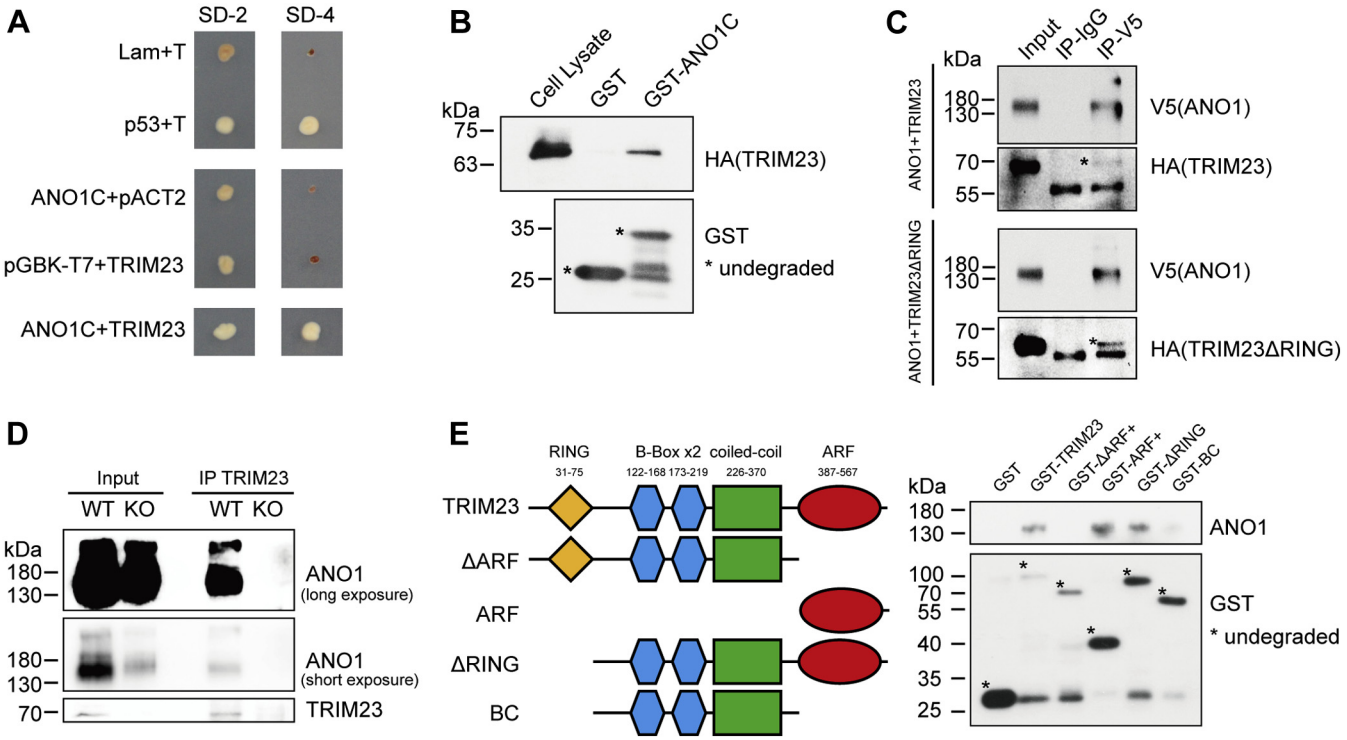

Figure 1. ANO1 physically interacts with TRIM23. *A*, ANO1 interacts with TRIM23 in yeast two-hybrid assays. The analyses included positive- and negative-control pairs (p53/T and Lam/T, respectively) and also tested for self-activation (*middle panel*). *B*, exogenous hemagglutinin (HA)-tagged TRIM23 in HEK293T cells was pulled down by GST–ANO1C but not GST alone. *C*, human ANO1–V5 was immunoprecipitated using the anti-V5 antibody or IgG (control) from HEK293T cells; both HA–TRIM23 (two *upper panels*) and HA–TRIM23ΔRING (two *lower panels*) coprecipitated with ANO1–V5. *D*, *lower* and *middle*, anti-TRIM23 antibody pulled down endogenous ANO1 together with TRIM23 from WT ZR-75-1 cells (WT) but not TRIM23 KO ZR-75-1 cells (KO). *Upper*, long exposure of the *middle panel*, to clearly show ANO1 absence in the Immunoprecipitation (IP) from TRIM23 KO cells. ANO1 was decreased in TRIM23 KO cells (see Fig. 2 and the main text). Ratio of input-to-IP sample loading: 1:45. *E*, various GST–TRIM23 truncation mutants were used to pull down purified ANO1 (*right*). *Left*, schematic of domains in various GST–TRIM23 mutants. *D* and *E*, the *asterisk* represents undegraded GST fusion protein or GST. All data in panels *B–E* are representative of three independent biological replicates. ANO1, anoctamin-1; ANO1C, ANO1 C terminus; IgG, immunoglobulin G; SD-2, synthetic defined media deficient in Leu and Trp; SD-4, Synthetic defined media deficient in Leu, Trp, His, and Ura; TRIM, tripartite motif.

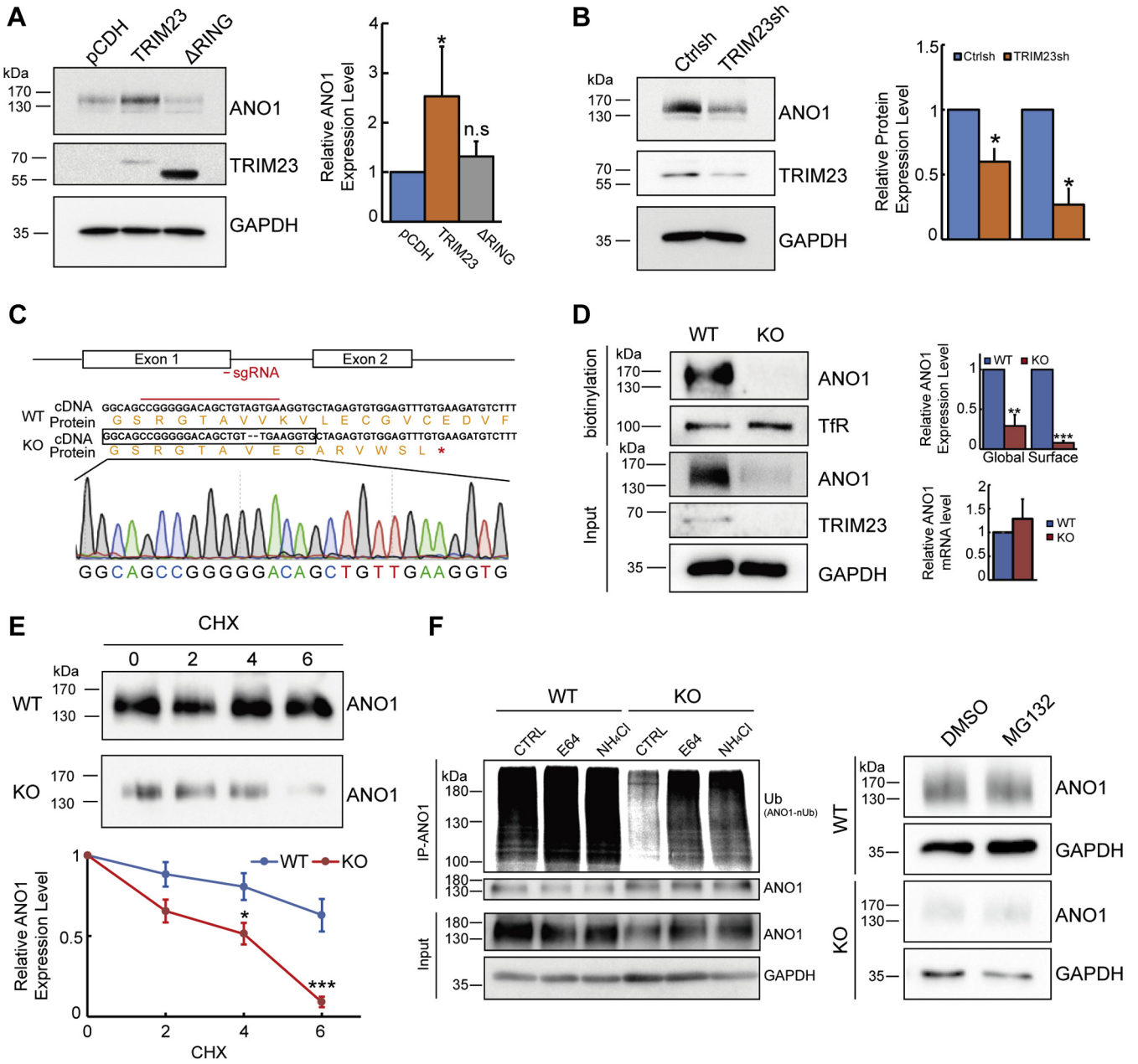

Figure 2. TRIM23 stabilizes ANO1 *in vitro*. *A*, *left*, expression of hemagglutinin–TRIM23 but not hemagglutinin–TRIM23ΔRING increased endogenous ANO1 in ZR-75-1 cells. pCDH, empty vector; GAPDH, loading control. *Right*, summary data of the *left panel*. Compared with control (pCDH), $*p = 0.032$, n = 5; ANOVA with Tukey's post hoc test used for statistical analysis. *B*, *left*, TRIM23 knockdown through RNAi attenuated ANO1 expression in ZR-75-1 cells. *Right*, summary data of the *left panel*. $*p \leq 0.026$, n = 4. *C*, schematic depicting generation of human TRIM23 KO ZR-75-1 cell line by using CRISPR/Cas9 techniques. Because of nonhomologous end joining, the use of a single-guide RNA (sgRNA) targeting exon 1 of human *TRIM23* caused homozygous deletion of 2 bp in exon 1, indicated by a *line* within the sgRNA region (*red line*); the deletion resulted in a reading-frame shift and a premature stop codon (indicated by *) in a cell clone. The TRIM23 KO clone was genotyped through DNA sequencing (*bottom*). *D*, TRIM23 KO ZR-75-1 cells exhibited undetectable TRIM23 expression (as expected) and showed marked downregulation of global and cell-surface ANO1 levels. Cell-surface ANO1 was biotinylated and isolated and then immunoblotted. qPCR results indicated no significant change in the ANO1 mRNA level in TRIM23 KO cells. $**p \leq 0.007$, n = 5 independent biological replicates; $***p = 0.0008$, n = 3; $p = 0.56$, n = 3. Transferrin receptor (TfR), positive control for cell-surface biotinylation. *E*, CHX assay of ANO1 in TRIM23 WT and KO ZR-75-1 cells. Cells were treated with 100 μM CHX for the indicated time. *Upper panel*, immunoblotting; *lower panel*, summary of immunoblotting results, normalized to the ANO1 level at 0 h. Different from WT, $*p < 0.03$, $***p < 0.0005$, n = 6. *F*, lysosomal inhibitors rescued ANO1 protein expression in TRIM23 KO but not WT ZR-75-1 cells. *Left*, cells were treated with lysosomal inhibitors NH_4Cl (25 mM) and E64 (10 μM) for 18 h; the inhibitors increased ANO1 protein expression level (input) and ubiquitination (IP-ANO1) in TRIM23 KO but not WT ZR-75-1 cells. Loading of immunoprecipitated ANO1 (IP-ANO1) in all lanes was equalized to clearly reveal differences in ANO1 ubiquitination. *Right*, cells were treated with proteasomal inhibitor MG132 (10 μM) for 18 h. Representative results from three independent experiments are shown in the *left* and *right panels*. Vehicle, DMSO. ANO1, anoctamin-1; CHX, cycloheximide; CRISPR/Cas9, clustered regularly interspaced short palindromic repeat/CRISPR-associated protein 9; Ctrlsh, control shRNA; DMSO, dimethyl sulfoxide; ns, not statistically significant; qPCR, quantitative PCR; RNAi, RNA interference; TRIM, tripartite motif; TRIM23sh, TRIM23 shRNA.

personal communication). Notably, in ZR-75-1 cells and in other cell types and tissues, ANO1 was heavily glycosylated, and the glycosylation was resistant to treatment with Endo H; this suggests that the glycosylation is processed by Golgi-mannosidase II and that most of the ANO1 protein is localized in the plasma membrane (Fig. S2*B*).

Next, the ANO1-binding region in TRIM23 was mapped; pull-down assays were performed to assess the interaction between ANO1 and GST-fusion constructs of four TRIM23 deletion mutants: (1) TRIM23 lacking the ARF+ domain (GST–ΔARF+, aa 1–402); (2) TRIM23 ARF+ domain [GST–ARF+, the ARF domain (aa 402–567) plus aa 568–574]; (3) TRIM23 lacking the RING domain (GST–ΔRING, aa 77–574); and (4) TRIM23 B-box domains (both domains) plus coiled-coil domain (GST–BC, aa 77–402) (Fig. 1*E*). The results indicate that the ARF+ domain (aa 402–574) is necessary and sufficient for interaction with ANO1, whereas the RING and B-box/B-box/coiled-coil domains are not involved in ANO1 binding (Fig. 1*E*). The co-IP results in Figure 1*C* also indicate that the RING domain is not required for ANO1 binding.

TRIM23 stabilizes ANO1 in vitro

To assess the functional impact of TRIM23 binding on ANO1, we examined ANO1 protein expression in the presence and absence of TRIM23. HA–TRIM23 was overexpressed in ZR-75-1 cells by using highly efficient lentivirus infection, but despite the overexpression, the HA–TRIM23 protein band appeared weak in immunoblotting (Fig. 2*A*); this agrees with previous reports and presumably reflects the self-ubiquitination–induced degradation also reported for several other E3 ubiquitin ligases (17). Unexpectedly, this apparently weak HA–TRIM23 expression was sufficient to cause a significant increase (∼2.5-fold) in the endogenous ANO1 protein level (Fig. 2*A*); by contrast, HA–TRIM23ΔRING, although expressed at a considerably higher level than HA–TRIM23, failed to enhance ANO1 expression (Fig. 2*A*). The higher HA–TRIM23ΔRING expression presumably resulted from the lack of E3 ligase activity and self-ubiquitination–induced degradation of the mutant protein. Notably, HA–TRIM23ΔRING can still bind to ANO1 (Fig. 1, *C* and *E*), which implies that the TRIM23 domains other than the RING domain are not involved in upregulating ANO1. Collectively, these results suggest that the E3 ligase activity of TRIM23 stabilizes ANO1 protein. Ubiquitination has been widely reported to perform nonproteolytic functions, including protein stabilization, in addition to producing its extensively studied proteolytic effect (18) (see Discussion).

To determine whether endogenous TRIM23 also exerts a stabilizing effect on ANO1, TRIM23 in ZR-75-1 cells was knocked down using RNA interference (RNAi): when ∼73% of TRIM23 was knocked down, ANO1 protein expression was decreased by ∼40% (Fig. 2*B*), which is consistent with the TRIM23 overexpression results (Fig. 2*A*). To more rigorously demonstrate the antiproteolytic effect of TRIM23 on ANO1 and facilitate further investigation of the underlying mechanism, a TRIM23 KO ZR-75-1 cell line was generated using clustered regularly interspaced short palindromic repeat (CRISPR)/CRISPR-associated protein 9 (CRISPR/Cas9) techniques (Fig. 2*C*). Homozygous TRIM23 KO ZR-75-1 cells expressed almost no detectable TRIM23, as expected, and showed nearly 70% to 90% reduction in global and cell-surface ANO1 expression (Fig. 2*D*). Notably, the ANO1 reduction was not likely due to any off-target effect of TRIM23 gene manipulation, in either RNAi-mediated knockdown or CRISPR/Cas9-mediated KO (Fig. 2, *B–D*), because distinct TRIM23 gene sequences were targeted in the two approaches (Experimental procedures). Furthermore, the ANO1 mRNA level was not markedly altered in TRIM23 KO cells (Fig. 2*D*), which implies post-transcriptional ANO1 regulation by TRIM23. Collectively, the results of these overexpression, knockdown, and KO experiments (Fig. 2) suggest that TRIM23 stabilizes global and cell-surface ANO1 through its RING domain.

TRIM23 slows ANO1 degradation

To ascertain how TRIM23 KO leads to a reduction in ANO1 protein levels, we used TRIM23 KO ZR-75-1 cells and performed the cycloheximide (CHX) chase assay, in which CHX treatment is used to block protein synthesis. When TRIM23 was knocked out, endogenous ANO1 degradation was substantially accelerated (Fig. 2*E*). Furthermore, in the absence of TRIM23, endogenous ANO1 appeared to be degraded mainly through a lysosomal pathway, as expected for the degradation of most ubiquitinated membrane proteins, because lysosomal but not proteasomal inhibitors elevated ANO1 expression in TRIM23 KO cells (Fig. 2*F*). By contrast, in WT cells, in which TRIM23 is present, the lysosomal inhibitors exerted little effect (Fig. 2*F*), which indicates that TRIM23 antagonizes ANO1 lysosomal degradation and thereby stabilizes ANO1. Moreover, treatment with the lysosomal inhibitors increased ANO1 ubiquitination in TRIM23 KO ZR-75-1 cells (Fig. 2*F*). These results indicate that an E3 ligase other than TRIM23 ubiquitinates ANO1 in TRIM23 KO ZR-75-1 cells and that the ubiquitination mediated by this E3 ligase leads to lysosomal degradation of ANO1; when ANO1 degradation in TRIM23 KO cells was blocked by the lysosomal inhibitors, ubiquitinated ANO1 was accumulated (Fig. 2*F*). In subsequent experiments (see below), we identified this additional ANO1-targeting E3 ligase as TRIM21.

TRIM23 ubiquitinates ANO1

Because the antiproteolytic effect of TRIM23 on ANO1 required the RING domain (Fig. 2*A*), we reasoned that TRIM23 stabilizes ANO1 by ubiquitinating ANO1 through its RING E3 ligase activity. Accordingly, HA–TRIM23 expression considerably elevated both the ubiquitination and the expression of ectopic ANO1–V5 protein in HEK293T cells (Fig. 3*A*); by contrast, HA–TRIM23ΔRING expression failed to increase ANO1–V5 ubiquitination or even moderately decreased it (presumably a dominant-negative effect resulting from competition with endogenous TRIM23) (Fig. 3*A*). These

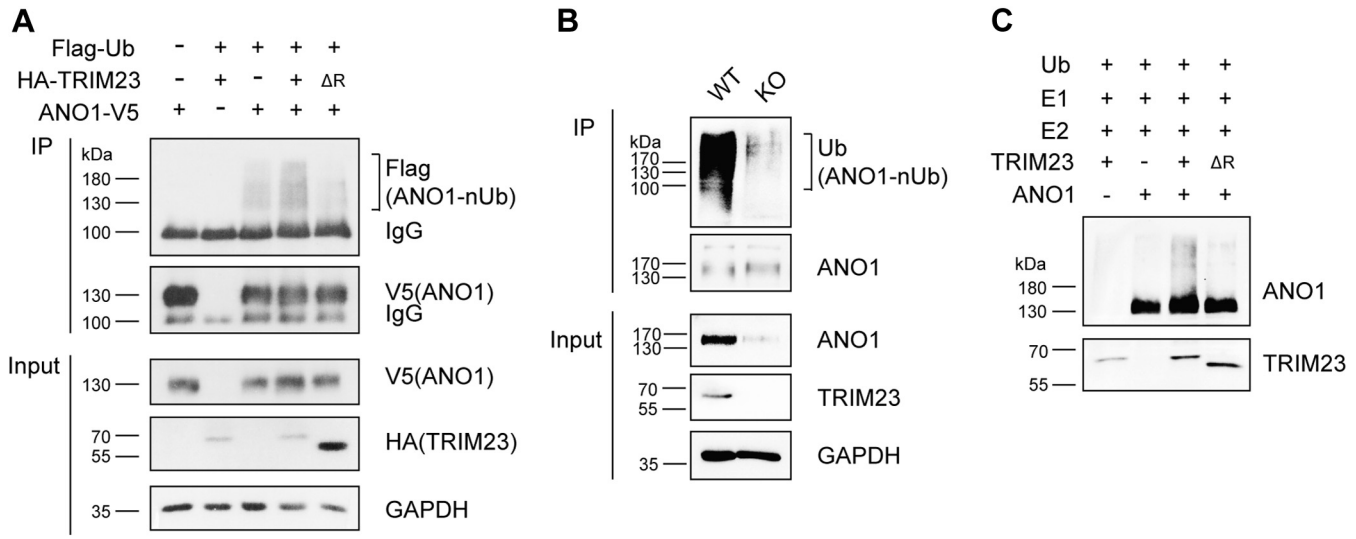

Figure 3. ANO1 is ubiquitinated by TRIM23. *A*, ANO1–V5, FLAG–Ub, and hemagglutinin–TRIM23 (or hemagglutinin–TRIM23ΔRING) were coexpressed in HEK293T cells. ANO1–V5 was immunoprecipitated with anti-V5 and immunoblotted with anti-FLAG. Loading of immunoprecipitated ANO1–V5 in all lanes was equalized to clearly reveal differences in ANO1 ubiquitination shown in panels *A* and *B*. *B*, endogenous ANO1 in TRIM23 WT and KO ZR-75-1 cells was immunoprecipitated with rabbit monoclonal anti-ANO1 and immunoblotted with mouse anti-ubiquitin. *C*, *in vitro* ubiquitination of ANO1 by TRIM23. Panels *A–C* are representative of 3 to 4 independent biological replicates. ΔR, TRIM23ΔRING; ANO1, anoctamin-1; ANO1–V5, V5-tagged full-length ANO1; E1, ubiquitin-activating enzyme; E2, UbcH5c; TRIM, tripartite motif; Ub, ubiquitin.

results suggest that TRIM23 ubiquitinates ANO1 through its RING E3 ligase and stabilizes ANO1 protein expression. Further supporting this notion, TRIM23 KO drastically lowered endogenous ANO1 ubiquitination in ZR-75-1 cells (Fig. 3*B*); moreover, these results appeared to indicate that ANO1 ubiquitination, at least in quiescent ZR-75-1 cells, was predominately mediated by TRIM23 but also involved another E3 ligase(s). To confirm that TRIM23 catalyzes ANO1 ubiquitination directly rather than through another E3 ligase, we assembled an *in vitro* ubiquitination system; here, addition of TRIM23 but not TRIM23ΔRING caused ANO1 ubiquitination (Fig. 3*C*). Collectively, these results (Fig. 3) clearly demonstrated that TRIM23 directly ubiquitinates ANO1 through its RING domain.

TRIM23 stabilizes ANO1 in vivo

We next addressed whether TRIM23 exerts an anti-proteolytic effect on ANO1 *in vivo* by knocking out *Trim23* in mice by using CRISPR/Cas9 techniques (Fig. 4*A*). No off-target mutation was detected in the seven top-scoring noncoding and coding regions that are potentially targeted by TRIM23 single-guide RNA (sgRNA) (Table S1).

ANO1 is known to be expressed in the dorsal root ganglion (DRG), salivary gland, lung, and heart; thus, we measured ANO1 expression in these tissues of TRIM23 KO mice by using a validated anti-mouse ANO1 antibody (ab53212, Abcam) (Fig. S1*B*). In TRIM23 KO mice, ANO1 protein level was halved in the DRG, salivary gland, and heart and reduced moderately (by ∼20%) in the lung (Fig. 4, *B* and *C*), which suggests that TRIM23 stabilizes ANO1 *in vivo*. By contrast, the transient receptor potential vanilloid 1 channel expression in the DRG was not altered in TRIM23 KO mice (Fig. S3), which indicates a specific effect of TRIM23 on ANO1. Similar to the results in TRIM23 KO ZR-35-1 cells (Fig. 2*D*), ANO1 mRNA showed no change in any of the examined TRIM23 KO tissues (Fig. 4*D*), which suggests that TRIM23 stabilizes ANO1 at the post-transcriptional level *in vivo* as well.

Functional impact of TRIM23–KO–induced ANO1 reduction

We evaluated the functional effect of TRIM23–KO–induced ANO1 protein reduction by using the DRG as an example tissue: We tested capsaicin-evoked pain sensation in mice because ANO1 has been implicated in DRG-mediated and chemical-induced pain sensation by us and others (19, 20). Strikingly, TRIM23 KO more than halved the total licking time in the capsaicin-induced pain-sensation assay, which suggests that TRIM23–KO–induced ANO1 protein reduction in DRG neurons influences chemical-/the transient receptor potential vanilloid 1-induced pain sensation (Fig. 4*E*). However, the reduction in pain sensation was not due to any change in the expression of the transient receptor potential vanilloid 1 (Fig. S3), the capsaicin receptor (19). Conversely, TRIM23 KO mice showed little difference in the von Frey filament experiment, which tests mechanical pain sensation and does not involve ANO1 (Fig. 4*F*).

Interestingly, TRIM23 KO also elevated the average heart rate by ∼21%, from 399 to 481 beats/min (Fig. 4*G*); this 21% increase is a physiologically drastic effect and is comparable with the changes induced by long-term exercising training, alteration of PKA expression, and neuropathic injury (21, 22, 23). This result suggests that ANO1 might hyperpolarize cardiomyocytes and reduce the heart rate under normal physiological conditions and further that TRIM23 KO decreases the ANO1 protein level (Fig. 4*C*) and thereby increases the heart rate (see Discussion).

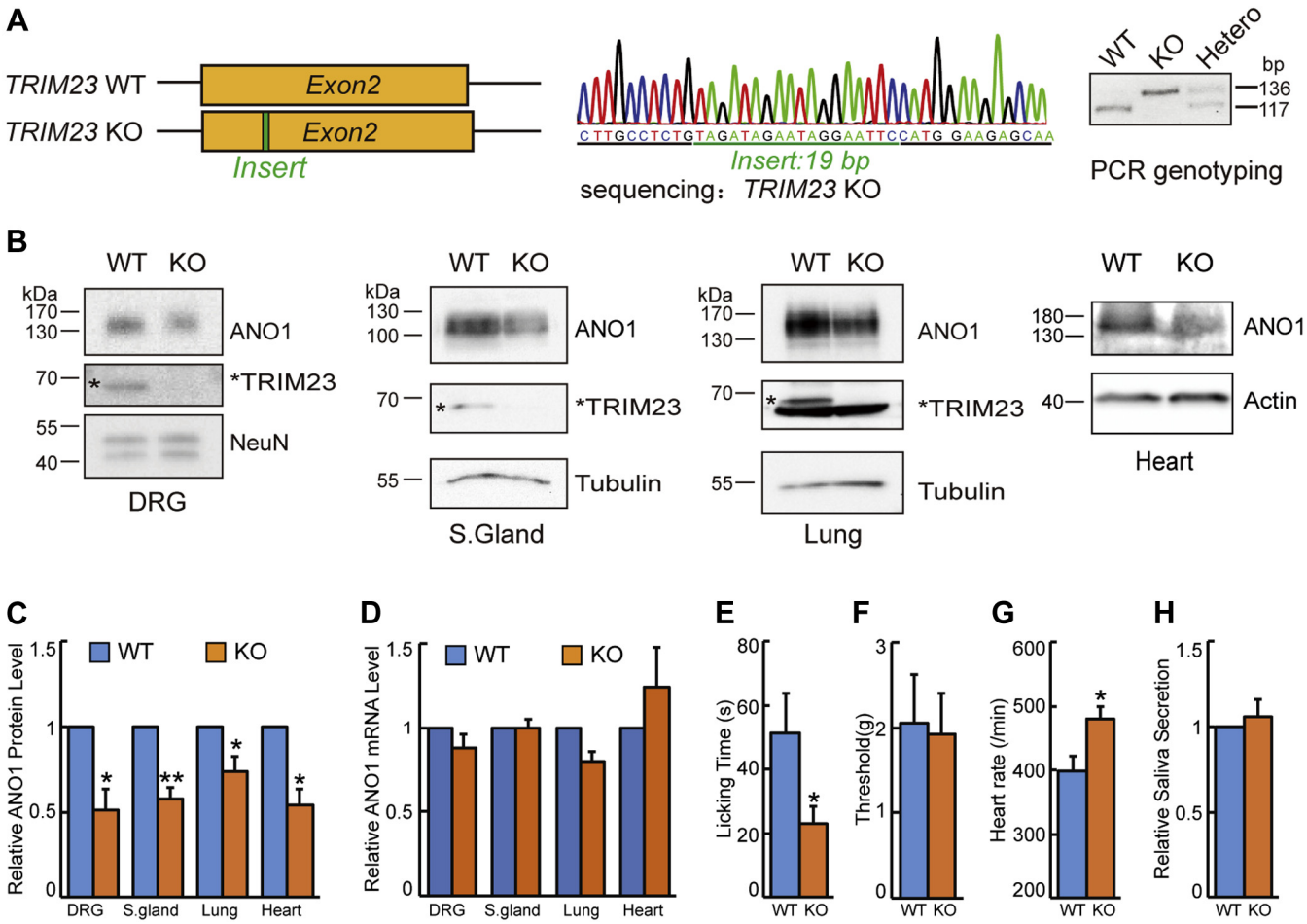

Figure 4. TRIM23 stabilizes ANO1 *in vivo*. *A*, schematic depicting generation of mouse line carrying a 19-bp insert in *Trim23* exon 2; the insert contains a stop codon and an EcoRI site (*left*). Gene KO was verified through DNA sequencing of *Trim23*$^{-/-}$ mice at first instance (*middle*), and subsequent genotyping was routinely performed using RT-PCR, which yielded a 19-nt insert in *Trim23*$^{-/-}$ (KO) mice (*right*). The EcoRI site in the 19-bp insert could be used for double-confirmation of genotypes. *B* and *C*, TRIM23 KO attenuated ANO1 expression in the DRG, salivary gland (S. Gland), lung, and heart. *C*, summary data of panel *B*. A nonspecific band was detected below TRIM23 in the lung tissue, and TRIM23 could not be resolved from Ig in the abundant blood present in heart tissue. Different from WT (*/**): DRG, $p = 0.0176$, n = 5; salivary gland, $p = 0.008$, n = 4; lung, $p = 0.016$, n = 9; heart, $p = 0.043$, n = 3. *D*, TRIM23 KO did not affect ANO1 mRNA expression in the DRG ($p = 0.20$, n = 5), salivary gland ($p = 0.94$, n = 6), lung ($p = 0.026$, n = 5), and heart ($p = 0.417$, n = 3). *E*, TRIM23 KO caused a reduction in chemical-induced pain sensation. *$p = 0.02$, n = 5. *F*, TRIM23 KO elicited no change in thresholds in von Frey filament assays. $p = 0.7$, n = 5. *G*, TRIM23 KO increased the heart rate by ~20%. *$p = 0.011$, n = 4. *H*, TRIM23 KO caused no change in relative saliva secretion. $p = 0.621$, n = 4 (WT/HE: three WT and one heterozygous). All panels: paired *t* test used for statistical analysis. ANO1, anoctamin-1; DRG, dorsal root ganglion; Ig, immunoglobulin; n, pair number of sex-matched littermates; TRIM, tripartite motif.

ANO1 has also been implicated in Ca^{2+}-dependent salivation (24). Because ANO1 expression was decreased in the salivary gland of TRIM23 KO mice (Fig. 4, *B–D*), we examined the salivation stimulated by pilocarpine, a muscarinic receptor agonist (25). However, we measured no notable change in salivation in TRIM23 KO mice (Fig. 4*H*) (see Fig. 6 and Discussion).

ANO1 interacts with another E3 ligase, TRIM21

A previous interactome study conducted using the cross-linker DSP suggested that ANO1 binds to TRIM21 E3 ubiquitin ligase (26), but little is known regarding whether and how TRIM21 E3 ligase modulates ANO1 function. We hypothesized that TRIM21 might mediate proteolytic ubiquitination of ANO1 and antagonize the TRIM23 function; this is because antiproteolytic ubiquitination of a protein by one E3 ligase (such as TRIM23) can be antagonized by the proteolytic ubiquitination by another E3 ligase (18, 27).

We first assessed whether TRIM21 physically interacts with ANO1, particularly the ANO1C: Xpress-tagged TRIM21 coprecipitated with ANO1–V5 from HEK293T cells (Fig. 5*A*), and Xpress-tagged TRIM21 was pulled down by GST–ANO1C but not GST alone (Fig. 5*B*). Moreover, endogenous TRIM21 and ANO1 expressed in ZR-75-1 cells coprecipitated in reciprocal co-IP experiments (Fig. 5*C*). Collectively, these results indicate that TRIM21 physically interacts with ANO1.

Notably, in contrast to TRIM23, TRIM21 moderately decreased ANO1 expression and concurrently increased ANO1 ubiquitination to a limited extent (Fig. 5*A*); this implies that TRIM21 destabilizes ANO1 through ubiquitination. The modest changes are probably due to the endogenous

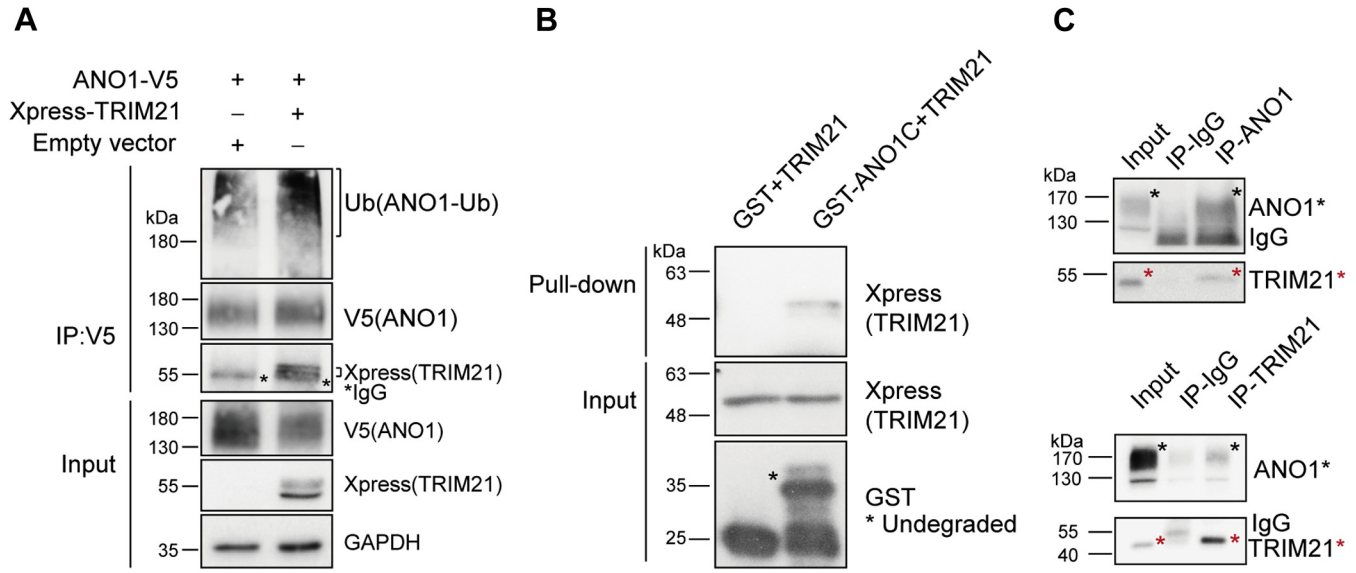

Figure 5. ANO1 physically interacts with TRIM21. *A*, human ANO1–V5 physically and functionally interacts with human Xpress–TRIM21 in HEK293T cells. Anti-Xpress antibody pulled down ANO1 together with Xpress–TRIM21 from cells coexpressing ANO1–V5 and Xpress-TRIM21 but not from cells expressing ANO1–V5 alone. TRIM21 expression also moderately lowered ANO1 protein expression and increased ANO1 ubiquitination to a limited extent. In IP, the *asterisk* denotes IgG; the *bracket* denotes TRIM21 doublet also detected in "Input." *B*, exogenous Xpress–TRIM21 in HEK293T cells was captured by GST–ANO1C but not GST alone. Results shown are representative of three independent biological replicates. The *asterisk* denotes undegraded GST or GST–ANO1. *C*, endogenous TRIM21 (*red* *) and ANO1 (*black* *) interact in ZR-75-1 cells. *Upper*, endogenous ANO1 was immunoprecipitated with anti-mouse ANO1 or control IgG and then immunoblotted with anti-ANO1 (*top*) and anti-TRIM21 (*bottom*). *Lower*, endogenous TRIM21 was immunoprecipitated with anti-TRIM21 or control IgG and then immunoblotted with anti-ANO1 (*top*) and anti-TRIM21 (*bottom*). All data in panels *A–C* are representative of three independent biological replicates. ANO1, anoctamin-1; ANO1–V5, V5-tagged full-length ANO1; ANO1C, ANO1 C terminus; Ig G, immunoglobulin G; TRIM, tripartite motif; Xpress-TRIM21, Xpress-tagged TRIM21.

expression of the antagonistic E3 ligase TRIM23 in the cells (see Fig. 3*A* and below).

TRIM21 destabilizes ANO1 in vitro *and* in vivo

We further examined how TRIM21 binding functionally affects ANO1. Similar to the results in HEK293T cells (Fig. 5*A*), HA–TRIM21 expression moderately lowered endogenous ANO1 expression in WT ZR-75-1 cells, which suggests that TRIM21 destabilizes ANO1 in ZR-75-1 cells (Fig. 6*A*). Notably, the destabilizing effect of TRIM21 was stronger in TRIM23 KO than WT ZR-75-1 cells (Fig. 6*A*), which indicates that TRIM23 antagonizes the destabilizing effect of TRIM21 on ANO1. In agreement with the TRIM21 overexpression results (Fig. 6*A*), RNAi-mediated knockdown of TRIM21 substantially increased endogenous ANO1 expression (by ∼2.6-fold) in ZR-75-1 cells (Fig. 6*B*).

We also measured the effect of TRIM21 KO on ANO1 protein expression *in vivo* by using *Trim21*$^{-/-}$ mice (in which *Trim21* is replaced with a GFP reporter): TRIM21 KO increased ANO1 expression nearly 3-fold in the salivary gland and by ∼40% in the heart (Fig. 6, *C* and *D*), which indicates that TRIM21 destabilizes ANO1 *in vivo*. However, TRIM21 KO did not alter ANO1 expression in the DRG or lung (Fig. S4). Intriguingly, TRIM21 KO did not affect ANO1 mRNA expression in the salivary gland but halved the expression in the heart (Fig. 6*C*); thus, TRIM21 downregulates salivary ANO1 expression at the post-transcriptional level but appears to exert a complex regulatory effect on cardiac ANO1 (see Discussion).

Studies conducted by us (not shown) and others have revealed that TRIM21 in mouse tissues cannot be readily detected with anti-TRIM21 antibodies, at least under normal physiological conditions (28), probably because of the self-ubiquitination–induced degradation of TRIM21. However, GFP-reporter expression in TRIM21 KO mice can reflect *Trim21* transcription and, by extrapolation, TRIM21 protein expression in specific tissues. Here, GFP expression in the salivary gland, heart, and lung, but not in the DRG, indicated potential TRIM21 protein expression in the three tested tissues other than the DRG (Fig. 6, *C* and *D* and Fig. S4). Thus, the lack of change in ANO1 expression in the DRG of TRIM21 KO mice can be attributed to the absence of TRIM21 expression (Fig. S4*A*); conversely, the absence of a TRIM21 effect on pulmonary ANO1 cannot be readily explained because the lung expressed GFP (Fig. S4*B*). A simple explanation is that the lung expresses little or no TRIM21 protein although it expresses GFP, a reporter of *Trim21* transcription. Nevertheless, our results (Fig. 6, *C* and *D* and Fig. S4) suggest that TRIM21 downregulates ANO1 expression *in vivo* in a tissue-specific manner.

Next, we examined the functional impact of TRIM21–KO–induced ANO1 upregulation. As before (Fig. 4*H*), we examined salivation in TRIM21 KO mice, which revealed a physiologically substantial increase (of ∼23%) (Fig. 6*D*); this ∼23% change is comparable with the salivation change induced by knocking out M3 muscarinic acetylcholine receptor (29). These results are consistent with the notion that TRIM21 regulates ANO1 expression and function in the salivary gland.

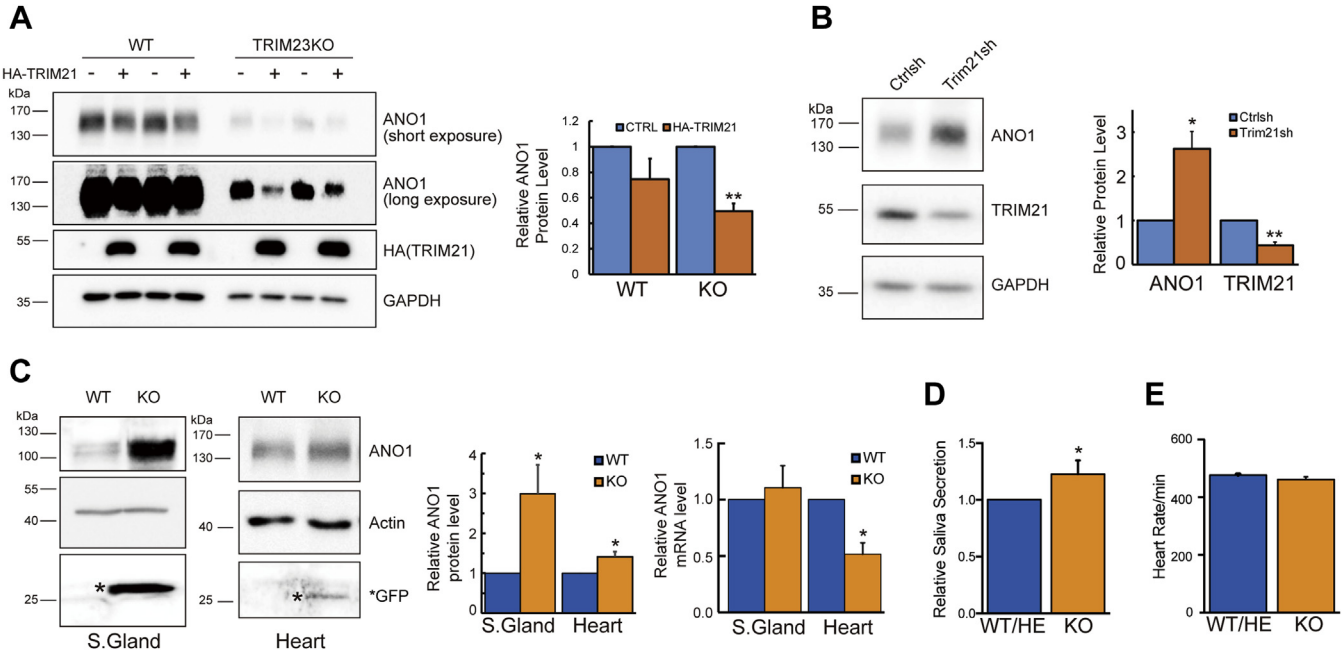

Figure 6. TRIM21 destabilizes ANO1. *A*, *left*, endogenous ANO1 was more markedly decreased after hemagglutinin–TRIM21 expression in TRIM23 KO than WT ZR-75-1 cells. Long and short exposures (*top half*) clearly show TRIM21 effect in TRIM23 WT and KO cells, respectively. GAPDH, loading control. *Right*, summary data of the left panel. $^{**}p = 0.0011$, n = 5. ANO1 expression was decreased in TRIM23 KO cells. Data are normalized to ANO1 expression without hemagglutinin–TRIM21 expression. *B*, *left*, TRIM21 knockdown through RNAi robustly elevated ANO1 expression in ZR-75-1 cells. *Right*, summary data of the *left panel*. $^{*}p = 0.03$ for ANO1, $^{**}p = 0.005$ for TRIM21, n = 4. *C*, TRIM21 KO increased ANO1 protein but not mRNA level in both the salivary gland and heart relative to the level in sex-matched WT littermates. GFP: reporter of *Trim21* transcription in TRIM21 KO mice. *Middle*, summary data of the *left panel*; *right*, summary data of mRNA levels. $^{*}p \leq 0.033$ (n = 7 for the salivary gland, n = 5 for the heart). For mRNA level, $p = 0.640$, n = 3 for the salivary gland; $p = 0.041$, n = 3 for the heart. *D*, TRIM21 KO increased saliva secretion in mice. $^{*}p = 0.032$, n = 4 (WT/HE: two WT and two heterozygous). *E*, the heart rate did not differ significantly between TRIM21 KO mice and their WT/HE littermates; $p = 0.259$, n = 5 (WT/HE: three WT and two heterozygous). ANO1, anoctamin-1; Ctrlsh, control shRNA; RNAi, RNA interference; TRIM, tripartite motif; TRIM21sh, TRIM21 shRNA.

By contrast, TRIM21 KO exerted no effect on the heart rate (Fig. 6*E*) (see Discussion).

EGF regulates ANO1 protein expression through TRIM23

In human colonic epithelial T84 cells, chronic EGF treatment was previously reported to upregulate ANO1 protein and mRNA levels, but the underlying molecular mechanism was not investigated in the study (5). Because TRIM23 was found to upregulate ANO1 (Figs. 2–4), we investigated whether EGF induction of ANO1 expression is mediated by TRIM23. EGF treatment substantially increased ANO1 protein expression in WT ZR-75-1 cells, and, notably, TRIM23 KO abolished the stimulatory effect of the EGF (Fig. 7*A*); this suggests that the EGF upregulates ANO1 expression through TRIM23. Conversely, EGF treatment exerted no effect on the ANO1 mRNA level (Fig. 7*B*), which was expected considering that TRIM23 was found to regulate ANO1 expression at the post-translational level in ZR-75-1 cells (Figs. 2*D* and 4*D*). This result agrees with previous results obtained in Te11 cells (30) but contradicts the aforementioned study in T84 cells, in which the EGF increased ANO1 mRNA expression (5). We repeated the experiments by using T84 cells to test whether this discrepancy might arise from a cell-type difference, but we found that the EGF markedly increased the ANO1 protein level but did not affect ANO1 mRNA expression in T84 cells (Fig. 7, *C* and *D*). Thus, the precise reason for the discrepancy between our result and the previous results in T84 cells remains unclear.

Because the stimulatory effect of the EGF was abolished by TRIM23 KO, we reasoned that the EGF modulates ANO1 ubiquitination. Intriguingly, EGF treatment significantly reduced ANO1 ubiquitination and concurrently increased ANO1 expression (Fig. 7, *E* and *F*). Moreover, the EGF-induced reduction in ANO1 ubiquitination was eliminated by TRIM23 KO (Fig. 7, *E* and *F*). These results indicate that EGF stimulation potentially blocks TRIM21-mediated ubiquitination of ANO1 through TRIM23 because only a reduction in TRIM21-mediated proteolytic ubiquitination was associated with an increase in ANO1 protein expression. However, TRIM23 and TRIM21 do not appear to physically compete for ANO1 binding (Fig. S5) (see Discussion).

Discussion

ANO1 stabilization by TRIM23

Here, we found that TRIM23 ubiquitinates—unexpectedly in a nonproteolytic manner—and stabilizes ANO1 protein expression in human ZR-75-1 cells and several mouse tissues (Fig. 8). TRIM23 has been reported to ubiquitinate and stabilize peroxisome proliferator-activated receptor γ (31) and to ubiquitinate NEMO (NF-kappa-B essential modulator) (nuclear factor kappa-B kinase subunit gamma) and NS5 protein of yellow fever virus and alter their function in a

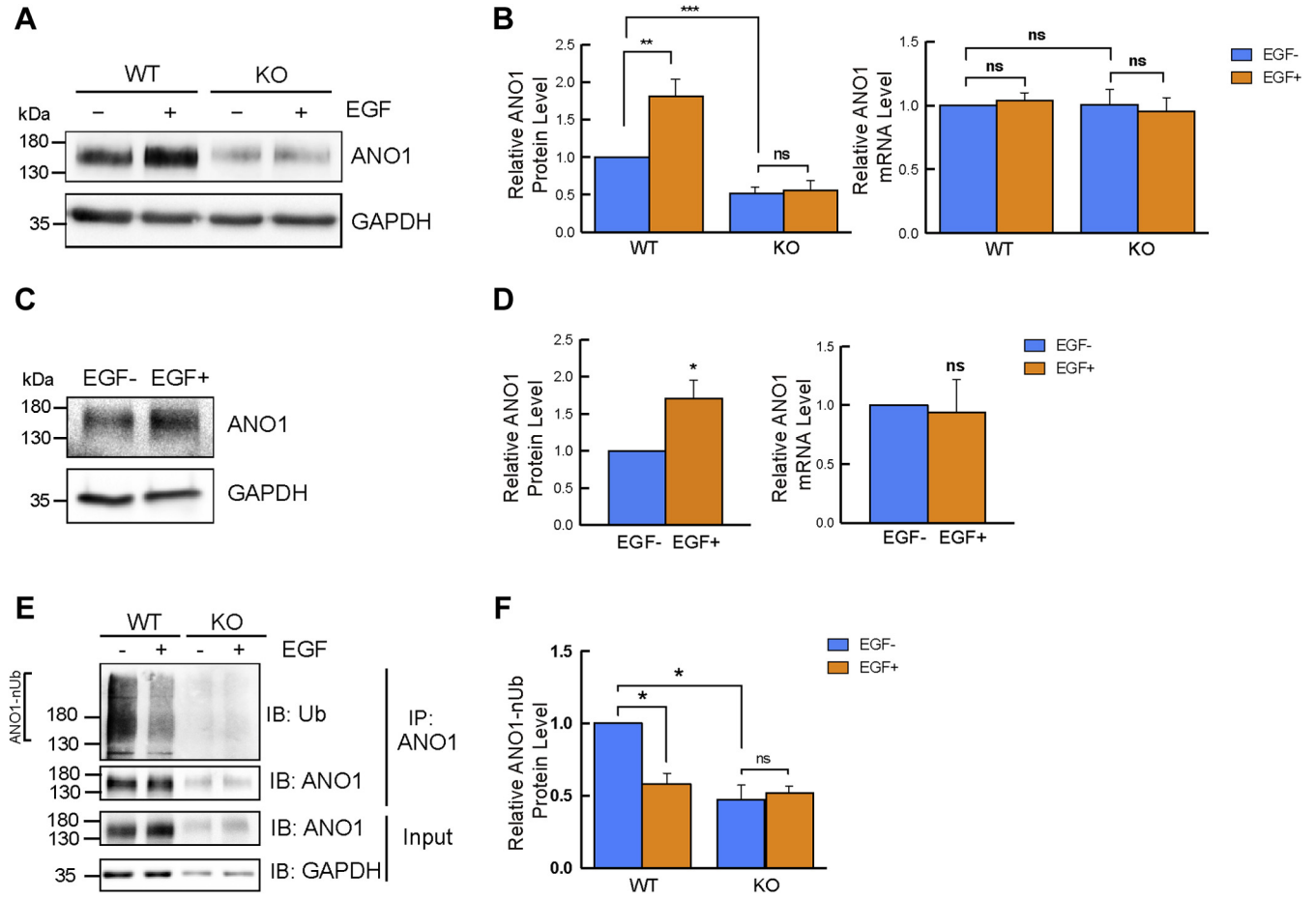

Figure 7. EGF regulates ANO1 through TRIM23. *A*, EGF treatment increased ANO1 expression in WT but not TRIM23 KO ZR-75-1 cells. GAPDH, loading control. *B*, summary data of panel *A* (*left*, n = 8), and qPCR analysis of ANO1 mRNA level of 4 of 8 independent biological repeats in the *left panel* (*right*, n = 4). $^{**}p = 0.0095$, $^{***}p = 0.0008$; *C*, EGF treatment increased ANO1 protein expression in T84 cells. *D*, summary data of panel *C* (*left*, n = 5) and qPCR analysis of ANO1 mRNA level of 4 of 5 independent biological repeats in the *left panel* (*right*, n = 4). $^{*}p = 0.0443$. *E*, EGF treatment significantly deceased ANO1 ubiquitination in WT but not TRIM23 KO ZR-75-1 cells. Immunoprecipitated ANO1 was equalized to clearly show differences in ANO1–nUb levels with/without EGF treatment. *F*, summary data of panel *E*. $^{*}p \leq 0.014$; ns, $p = 0.684$; n = 4. In panels *A–D*, both ANO1 protein and mRNA levels were normalized to GAPDH levels; in panel *F*, ANO1–nUb level was adjusted to immunoprecipitated ANO1. ANO1, anoctamin-1; EGF, epidermal growth factor; ns, not statistically significant; nUb, polyubiquitination; qPCR, quantitative PCR; TRIM, tripartite motif.

nonproteolytic manner (32, 33). Collectively, our work and the previous studies suggest that TRIM23 E3 ligase predominantly mediates nonproteolytic ubiquitination, except for self-ubiquitination–induced degradation (Fig. 2*A*).

Besides producing its well-known proteolytic effect, ubiquitination performs nonproteolytic functions, such as modulation of membrane trafficking, protein kinase activation, DNA repair, and regulation of chromatin dynamics (34). Furthermore, emerging evidence, including the aforementioned study on peroxisome proliferator-activated receptor γ, has now extended the nonproteolytic function of ubiquitination to protein stabilization. For example, an atypical E3 ligase,

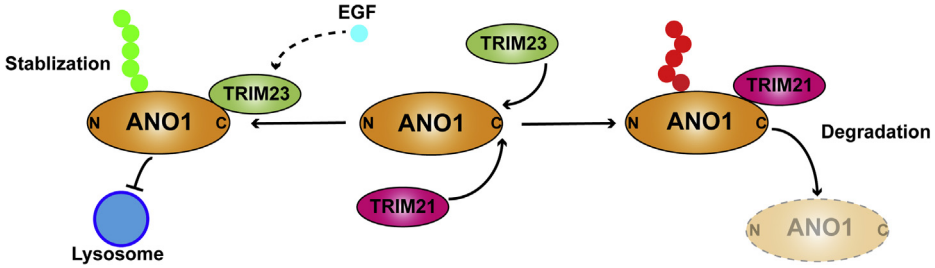

Figure 8. Schematic showing ANO1 regulation by antagonistic TRIM23 and TRIM21 E3 ligases. Both TRIM23 and TRIM21 bind to ANO1 C terminus. TRIM23 ubiquitinates and stabilizes ANO1 by preventing lysosomal degradation, whereas TRIM21 ubiquitinates and causes ANO1 degradation. EGF signaling enhances ANO1 expression through TRIM23 by a mechanism that remains unclear but potentially involves blocking of TRIM21 ubiquitination of ANO1 (rather than blocking of TRIM21 to the same site—ANO1 C terminus). *Green* and *red dots*, antiproteolytic and proteolytic ubiquitination. ANO1, anoctamin-1; EGF, epidermal growth factor; N and C, N- and C-termini; TRIM, tripartite motif.

zinc finger protein 91, stabilizes nuclear factor kappa-light-chain-enhancer of activated B cells-inducing kinase (35); the E3 ligase FBXL21 regulates oscillation of the circadian clock through ubiquitination and stabilization of cryptochromes and antagonizes the proteolytic effect of another E3 ligase, FBXL3 (18, 27); UHRF2 of the RING-domain family ubiquitinates and stabilizes the acetyltransferase TIP60 (36); and TRIM21 appears to stabilize keratin 17 (37). Notably, zinc finger protein 91, UHRF2, and TRIM21 also mediate the proteolytic ubiquitination of other protein targets (36, 38) (see below for TRIM21), and these studies therefore imply that stabilization or antiproteolytic ubiquitination is not mediated by specifically designated E3 ligases.

Because the observed stabilizing effect of TRIM23 on ANO1 was an unexpected finding, we used multiple complementary approaches to confirm the effect: (1) TRIM23 overexpression in ZR-75-1 cells (Fig. 2*A*); (2) TRIM23 knockdown in ZR-75-1 cells by using RNAi (Fig. 2*B*); (3); TRIM23 KO in ZR-75-1 cells by using CRISPR/Cas9 techniques (Fig. 2, *C* and *D*); (4) treatment of WT and TRIM21 KO ZR-75-1 cells with lysosomal inhibitors (Fig. 2*D*); and (5) TRIM23 KO in mice by using CRISPR/Cas9 techniques. Collectively, the results of these experiments involving distinct approaches corroborated each other and clearly demonstrated the stabilizing effect of TRIM23 on ANO1. Notably, lysosomal inhibitors produce broad and nonspecific effects on all proteins that are susceptible to lysosomal degradation, including proteins involved in ubiquitination signaling; because this complicates data interpretation, the results of experiments in which these inhibitors are used must be interpreted with caution, particularly in the absence of other corroborating evidence.

ANO1 degradation induced by TRIM21

Another key finding here is that TRIM21 E3 ligase, a paralog of TRIM23, ubiquitinates and causes ANO1 degradation in human ZR-75-1 cells and mouse tissues (Fig. 8). TRIM21 is a multifunctional protein and its role as an intracellular antibody receptor in immune responses has been extensively studied. As an E3 ligase, TRIM21 targets several substrates involved in innate and adaptive immunity and cancer development, including sequestosome 1 (SQSTM1/p62) (39), mitochondrial antiviral signaling protein (40), and multiple members of the interferon regulation factor (IRF) protein family (IRF3/5/7/8) (41–44). Our study has identified ion channels as a target of TRIM21 E3 ligase for the first time.

Antagonistic TRIM23 and TRIM21 control ANO1 expression and physiological functions

Interestingly, the proteolytic effect of TRIM21 on ANO1 was antagonized by the ubiquitination of ANO1 by TRIM23 in human ZR-75-1 cells (Figs. 6*A* and 8). Similar results were also obtained in the mouse salivary gland and heart: TRIM23 KO decreased ANO1 protein expression (Fig. 4, *B–D*), whereas TRIM21 KO increased ANO1 expression (Fig. 6*C*). This control of ANO1 protein homeostasis by two antagonistic E3 ligases is reminiscent of the effect of FBXL21 and FBXL3 on cryptochromes (18, 27). TRIM21 regulation of cardiac ANO1 expression was multilevel and complex: TRIM21 KO moderately increased ANO1 protein expression but decreased ANO1 mRNA expression (Fig. 6*C*). Conceivably, the transcriptional downregulation dampened a post-transcriptional upregulation, and this might represent a protective negative-feedback mechanism for preventing TRIM21 reduction from inducing excessive ANO1 expression, which would lead to potentially fatal bradycardia (Fig. 4, *C* and *G*).

The antagonistic effects of TRIM23 KO and TRIM21 KO on ANO1-mediated physiological functions were less overt than their effects on ANO1 protein expression in the salivary gland and heart. In the salivary gland, TRIM23 KO decreased ANO1 protein expression by 50% (Fig. 4, *B–D*), whereas TRIM21 KO caused an almost 3-fold increase in ANO1 protein expression (Fig. 6*C*); thus, TRIM21 KO significantly stimulated saliva secretion (Fig. 6*D*), whereas TRIM23 KO exerted no effect (Fig. 4*H*). In the heart, TRIM23 KO decreased ANO1 protein expression by ∼50% (Fig. 4, *B–D*) and TRIM21 KO increased ANO1 protein expression by ∼40% (Fig. 6*C*); consequently, TRIM23 KO significantly elevated the heart rate (Fig. 4*G*) but TRIM21 KO produced a negligible effect (Fig. 6*E*). One simple explanation for the lack of physiological effects might be that the change in ANO1 level in KO mice relative to the level in WT mice is not adequately large to produce readily measurable physiological alterations. Further investigation will be required to address whether changes in ANO1 protein expression, even when causing no apparent physiological changes on their own, could produce a notable physiological impact when the physiologically subthreshold ANO1 changes become sufficiently large under certain pathological conditions or when several such alterations act cumulatively and synergistically.

Chloride channels play critical yet complex roles in the modulation of cardiac functions (45). ANO1 mRNA and protein are suggested to be expressed in cardiomyocytes, and ANO1 activation might contribute to early phase 1 repolarization of action potentials, according to pharmacological studies (46). However, the effect of genetic manipulation of cardiac ANO1 has not been studied to date; this is because global ANO1 KO in mice leads to extremely poor survival, and conditional cardiac ANO1 KO mice are unavailable. Our TRIM23 KO mice serve as an ANO1 knockdown model and enable examination of the effect of cardiac ANO1 manipulation. Our results revealed that ANO1 reduction significantly elevated the heart rate (Fig. 4*C*), which appears to agree with the general effect of chloride channel activation on the hyperpolarization of action potentials (45). Nevertheless, our study suggests that ANO1 plays a crucial role in the modulation of cardiac function.

TRIM23 and TRIM21 expression in DRG neurons and the lung

Both the DRG and the lung expressed TRIM23, and TRIM23 KO attenuated ANO1 protein expression in the two tissues (Fig. 4, *B* and *C*). Moreover, TRIM23–KO–induced ANO1 protein reduction drastically altered chemical-induced

pain sensation. By contrast, the lung, but not the DRG, appeared to express TRIM21, according to GFP-reporter expression (Fig. S4), although GFP expression does not guarantee ANO1 expression (Fig. S4*B*). However, TRIM21 KO exerted no effect on ANO1 protein expression in either the DRG or the lung. Collectively, these results suggest that TRIM23 and TRIM21 expression and functions are not unfailingly paired in the same tissue or cell type, at least under normal physiological conditions. Whether this also holds under certain pathological conditions remains to be explored.

TRIM23 links ANO1 regulation with the EGF and other physiological modulators

The EGF is a key regulator of the growth, migration, differentiation, and electrolyte secretion (5) of numerous cell types. Chronic EGF treatment was suggested to upregulate ANO1 protein and mRNA levels in epithelial T84 cells (5); presumably, the observed EGF effects on cell growth and electrolyte secretion were at least partially mediated by the stimulatory effect of the EGF on ANO1 protein expression, because ANO1 also regulates cell growth and electrolyte secretion, at least in epithelial cells. However, the molecular mechanism underlying EGF regulation of ANO1 was not investigated in the previous study (5). Our results suggest that EGF upregulates ANO1 protein expression through TRIM23 in ZR-75-1 cells, with EGF stimulation potentially suppressing TRIM21-mediated ubiquitination of ANO1 through TRIM23 (Figs. 7 and 8). Further investigation is required to determine precisely how the EGF produces this effect. One possibility is that EGF signaling might directly cause TRIM23 phosphorylation, and the phosphorylation of TRIM23 might prevent TRIM21 from binding to ANO1 because both TRIM23 and TRIM21 bind to the same small region of ANO1: ANO1C (aa 904–986 of the acd isoform). However, our data suggest that TRIM23 and TRIM21 do not physically compete for ANO1 binding (Fig. S5). Another possibility is that EGF signaling leads to the phosphorylation of ANO1 and thus promotes the subsequent TRIM23-mediated ubiquitination of ANO1, especially considering that protein phosphorylation is widely recognized to serve as a cue for the ubiquitination of proteins. TRIM23-induced ubiquitination might then prevent TRIM21-induced ubiquitination of ANO1 without blocking TRIM21 binding to ANO1.

EGF signaling, including EGF secretion and EGF receptor expression, is tightly regulated by a wide array of signaling molecules, including estrogen/androgen (47), growth hormone (48), and calcitriol/parathyroid hormone (49). Therefore, our findings regarding the EGF–TRIM23 signaling axis indicate that TRIM23 might play a critical role in ANO1 regulation by several other physiological modulators.

TRIM21/TRIM23 regulation of ANO1: Association with diseases

TRIM21 increase has been implicated in inflammation (50, 51). For instance, three proinflammatory interferons (α, β, and γ) were reported to stimulate TRIM21 transcription through IRF1 and IRF2 and elevate ANO1 protein expression in immune cells; more importantly, TRIM21, IRF1, and IRF2 were all found to be upregulated in the immune cells of patients with the autoimmune disease Sjogren's syndrome (51). If TRIM21 expression in the salivary gland also increases in Sjogren's syndrome and inflammation, both ANO1 protein expression in the salivary gland and salivation would be expected to decrease (Fig. 6, *C* and *D*) (24); intriguingly, decreased salivation is a signature symptom of Sjogren's syndrome. Thus, it would be of interest to investigate whether salivary TRIM21 and ANO1 are altered in Sjogren's syndrome.

ANO1 mRNA and protein levels have long been known to be upregulated in numerous cancers, such as breast cancer, HNSCC, and colorectal cancer, and ANO1 upregulation is associated with disease grade and poor prognosis in several cancers (6, 52). ANO1 increase, rather than being merely a consequence or by-product of tumorigenesis, actively regulates tumorigenesis: suppression of ANO1 expression or channel activity has been found to decrease tumor formation (6, 52, 53). ANO1 overexpression in cancer results from the amplification of chromosomal locus 11q13 in certain but not all cases (6, 52).

Notably, decreased TRIM21 protein and mRNA expression has also been linked to several cancers. For example, TRIM21 suppresses colorectal and breast cancers by ubiquitinating and causing the degradation of, respectively, serine hydroxymethyltransferase 2 (44) and the transcription factors Sal-like proteins 1 and 4 (42); moreover, TRIM21 downregulation in breast cancer is closely correlated with the large tumor size and poor prognosis (54). Conversely, elevated TRIM23 expression has been suggested to be associated with poor prognosis in gastric cancer (55) and HNSCC (56). These opposite effects of TRIM21 and TRIM23 on tumorigenesis appear to agree closely with their antagonistic modulation of the homeostasis of ANO1 protein, the overexpression of which promotes tumorigenesis. Thus, mutation or altered expression of TRIM21 or TRIM23 could represent a previously unidentified mechanism underlying ANO1 upregulation in cancer cells. Aberrant ubiquitin-dependent regulation of ion channels has long been known to be associated with human diseases such as Liddle syndrome (57).

Experimental procedures

Antibodies

The following commercially available antibodies were used: rabbit monoclonal anti-human ANO1 (ab64085) and rabbit polyclonal anti-mouse ANO1 (ab53212), Abcam; rabbit anti-human/mouse TRIM23 (HPA-039605) and mouse anti-FLAG (F1804), Sigma-Aldrich; mouse anti-HA (MMS-101P), Covance Research Products Inc; mouse anti-V5 (P/N-46-0705) and anti-Xpress (R910-25), Invitrogen; and mouse anti-human TRIM21 (sc-25351), anti-ubiquitin (sc-8017), anti-GAPDH (sc-365062), and anti-actin (sc-47778), Santa Cruz Biotechnology.

Yeast two-hybrid assays

Yeast two-hybrid assays were performed to screen for E3 ligases that bind to ANO1, as described previously (16). Briefly, the C-terminal 83 amino acid residues of human ANO1 (aa 904–986 of the acd isoform, ANO1C) were used as a bait to screen a homemade library comprising >300 human E3 ligases (16).

Cell culture and transfection

HEK293T cell line (RRID: CVCL_1926), human breast cancer cell line ZR-75-1 (RRID: CVCL_0588), and human colon epithelial cell line T84 (RRID: CVCL_0555) were obtained from American Type Culture Collection. The cells were assumed to be authenticated by American Type Culture Collection and were not further authenticated in this study. All cell lines were routinely tested and confirmed to be negative for *Mycoplasma* contamination. The cells were maintained in culture medium supplemented with 10% or 5% fetal bovine serum (FBS) (for T84) and 100 U/ml penicillin/streptomycin (Life Technologies) in an atmosphere of 95% air–5% CO_2 at 37 °C; Dulbecco's modified Eagle's medium (DMEM) was used for culturing HEK293T cells, Improved Minimum Essential Medium (IMEM) for ZR-75-1 cells, and DMEM:Nutrient Mixture F-12 for T84 cells. HEK293 T cells were transfected using 1 mg/ml polyethylenimine.

Viral gene transfer of ZR-75-1 cells for knockdown and overexpression

For TRIM23/TRIM21 knockdown in ZR-75-1 cells, a double-stranded shRNA oligo targeting TRIM23 (AAGAAATGGCTCTAAGTGT), TRIM21 (GCAGCAC GCTTGACAATGA), or a control sequence unrelated to TRIM23/TRIM21 (ACGCATGCATGCTTGCTTT) was cloned into the lentivirus transduction vector pLVTH (plasmid 12262; Addgene) to generate the plasmid construct pLVTH–TRIM23sh, pLVTH–TRIM21sh, or pLVTH–Ctrlsh, respectively. GFP, as an indicator of shRNA expression, was also cloned in pLVTH under the control of a separate promoter.

Lentiviruses were prepared by transfecting one of the three plasmids together with psPAX2 and pMD2G-VSVG (both from Addgene) into HEK293T cells. On post-transfection day 3, the culture medium containing the virus was filtered through a porous membrane (pore size, 0.45 μm), concentrated through ultracentrifugation (50,000*g*), and stored at −80 °C. For viral transfer, 1 ml of the concentrated lentivirus soup was added together with 8 μg/ml Polybrene to a 35-mm dish of 50%-confluent ZR-75-1 cells and incubated for 12 h; the virus-containing medium was then replaced with a fresh medium, and the culture was continued for another 12 h. After three repetitions of sequential viral infection, the culture was examined for GFP expression, which was typically detected in 80% to 90% of the cells.

For overexpressing human TRIM21, human TRIM23 (α isoform), and their mutants in ZR-75-1 cells, the corresponding cDNAs were cloned into the lentivirus transduction vector pCDH (CD510-1; System Biosciences). Lentiviruses were prepared using procedures similar to those mentioned above. After lentivirus infection of ZR-75-1 cells for 72 h, the virus soup was replaced with the fresh IMEM and the cells were cultured for 24 h before replacing the medium with the IMEM containing 2 μg/ml puromycin (Thermo Fisher) to select for positive transfection. After culturing for another 48 h, the remaining live cells were collected for Western blotting.

TRIM21 KO mice

TRIM21 KO mice were purchased from The Jackson Laboratory (C57BL/6-Trim21tm1Hm/J, Stock #010724) and genotyped according to a published protocol (58). All animal procedures in this or other sections were approved by the University Committee on Research Practices of the Hong Kong University of Science and Technology (Ethics protocol number: 2016074).

Generation of TRIM23 KO ZR-75-1 cells

TRIM23 KO ZR-75-1 cells were generated as follows: A target sequence in the first exon of human *TRIM23* (CCGGGGGACAGCTGTAGTGA; nt 146–165 in human TRIM23 transcript) was selected using online software (www.crispr.mit.edu), and the corresponding oligonucleotide was cloned into the BsmBI site of lentiCRISPR v2 (Addgene); this TRIM23-targeting plasmid was transfected into ZR-75-1 cells by using Lipofectamine 2000. At 48 h after transfection, the cells were selected for resistance to 4 μg/ml puromycin for 48 h and then resuspended (at 100 cells/ml) in the IMEM containing 10% FBS. Single colonies were hand-picked at 14 days after seeding. TRIM23 KO was identified by DNA sequencing and Western blotting.

Generation of TRIM23 KO mice

TRIM23 KO mice were generated using CRISPR/Cas9 genome-editing techniques. Briefly, a 20-bp guide sequence (CGTATTGCTCTTCCATGCAG) targeting *TRIM23* exon 2 was cloned into pSpCas9(BB) (plasmid 42230; Addgene) following a reported protocol (59, 60). Subsequently, Cas9 mRNA and TRIM23-targeting sgRNA were produced through *in vitro* transcription by using mMESSAGE mMACHINE T7 ULTRA and MEGAshortscript T7 kits (Life Technologies), respectively; both Cas9 mRNA and the sgRNA were purified using a MEGAclear Kit (Life Technologies). A single-stranded DNA oligo (ordered as Ultramer DNA oligos from Integrated DNA Technologies) was used as the donor for homology-directed repair; the oligo included a 19-nt insert (TAGATA GAATAGGAATTC), which contained three stop codons in different reading frames and an endonuclease EcoRI site, and two 60-nt arms.

Different concentrations of the Cas9 mRNA, sgRNA, and donor oligo, as reported previously (59), were mixed and injected into 200 fertilized eggs of C57BL/6 mice, and the eggs were subsequently transferred into the uterus of pseudo-pregnant female mice. The resulting newborn mice were genotyped using PCR: the sgRNA-targeted region in genomic

DNA (extracted from ear-punch samples) was amplified to determine whether it contained the 19-nt insert; positive PCR results were further confirmed through DNA sequencing.

GST pull-down and co-IP assays

For GST pull-down assays, GST fusion proteins were generated as described previously (61) and affinity-purified using Glutathione-Sepharose beads. Purified GST fusion proteins (or control GST) immobilized on Glutathione-Sepharose beads were incubated at 4 °C overnight with either whole-cell lysates of transfected HEK293T cells or purified human ANO1–His protein (see below). Subsequently, the beads were spun down and washed thrice with 3 ml of PBS containing 0.5% Triton X-100, and the captured proteins were eluted with SDS-PAGE loading buffer and analyzed by Western blotting.

Co-IP assays were performed using procedures described previously (62, 21), with a few modifications. Briefly, cells were lysed in a co-IP lysis buffer (20 mM Hepes, 175 mM NaCl, 0.5% NP-40, 10% glycerol, 1 mM EDTA, 1 mM DTT, and 1 mM PMSF, pH 7.6 adjusted with NaOH) supplemented with 1× cOmplete protease-inhibitor cocktail (Roche). After centrifugation, 1 μg of the antibody and 25 μl (bed volume) of Protein G beads (GE Healthcare) were added to ∼100 to 200 μg of whole-cell extracts, and the mixture was incubated at 4 °C overnight. The beads were washed thrice with 700 μl of the co-IP lysis buffer and then the immunocomplexes were collected for Western blotting.

CHX treatment

WT and TRIM23 KO ZR-75-1 cells were treated with 100 μM CHX (Sigma) dissolved in the culture medium for 2, 4, or 6 h, and the cells were then lysed in the radioimmunoprecipitation assay buffer (150 mM NaCl, 1.0% NP40, 0.5% sodium deoxycholate, 0.1% SDS, and 50 mM Tris, pH 7.4) supplemented with 1× protease-inhibitor cocktail (Roche). Cell lysates were subject to Western blotting.

In vitro *and* in vivo *ubiquitination assays*

In vitro ubiquitination assays were performed following described procedures and using an *in vitro* ubiquitination kit (BML-UW9920-0001, ENZO Life Sciences) (16). Briefly, 2.5 μg of purified ANO1–His was incubated with the components of the putative ubiquitination machinery: 100 ng of Uba1 (E1, ubiquitin-activating enzyme), 150 ng of UbcH5c (E2, ubiquitin-conjugating enzyme), 0.5 μg of purified 6His–TRIM23, and 5 μg of ubiquitin in a 50-μl (final volume) reaction buffer containing 25 mM Tris HCl, pH 7.6, 5 mM $MgCl_2$, 100 mM NaCl, 1 mM DTT, and 2 mM ATP. The mixture was incubated at 30 °C for 4 to 6 h, and the reaction was terminated by adding 1× SDS-PAGE loading buffer. Ubiquitination of ANO1–His was analyzed by immunoblotting with anti-ANO1. ANO1–His and 6His–TRIM23 were purified from HEK293T cells according to our previously described protocols (21), and the other proteins used here were supplied with the assay kit.

For *in vivo* ubiquitination assays of endogenous ANO1, WT or TRIM23 KO ZR-75-1 cells were lysed in the co-IP buffer and the lysates were centrifuged at 16,000*g* for 15 min at 4 °C; the expression of each protein of interest was confirmed by immunoblotting 10% of the collected supernatants, and the remaining supernatants were incubated with 1 μg of anti-ANO1 antibody and 20 μl of Protein G Sepharose (GE Healthcare) at 4 °C overnight. IP experiments were performed in the co-IP buffer supplemented with 1× protease-inhibitor cocktail (Roche) and 20 mM N-ethylmaleimide (E3876; Sigma). The recovered beads were washed thrice with the co-IP buffer supplemented with 0.5% Triton X-100 and heated in the SDS-PAGE loading buffer at 95 °C for 5 min, and the eluted proteins were immunoblotted with anti-ANO1 (ab64085; Abcam) or anti-ubiquitin. Similar procedures were used for the ubiquitination assay performed on ectopic ANO1 in HEK293T cells.

EGF treatment

WT and TRIM23 KO cells maintained in the IMEM containing 10% FBS were rebalanced with the IMEM without FBS for 1 h immediately before experiments, washed with PBS, and treated with the IMEM containing 100 ng/ml human recombinant EGF (Gibco) for 30 min. For protein analysis, cells were washed again with PBS, cultured in the IMEM containing 10% FBS for 8 h, and lysed in radioimmunoprecipitation assay buffer supplemented with 1× protease inhibitor cocktail (Roche) to obtain extracts for Western blotting. For quantitative RT-PCR analysis, cells were washed with PBS and cultured with the IMEM plus 10% FBS for 4 h, and then RNA was isolated using a total RNA extraction kit (below).

Quantitative real-time PCR

Total RNA was extracted using an RNA extraction kit (Minibest Universal RNA Extraction Kit, Takara), and cDNA was synthesized using Superscript II reverse transcriptase (Invitrogen). Quantitative PCR (qPCR) amplifications of various genes were performed using SYBR Green (Takara) and an ABI 7500 Fast Real-Time PCR System (Applied Biosystems); GAPDH was used as a normalization control. After initial denaturation (30 s, 95 °C), amplification was performed using 40 cycles of 5 s at 95 °C and 34 s at 60 °C. All qPCR data represent the means ± SEM.

The sequences of the primers used for qPCR were the following: hANO1: 5′-CTCCTGGACGAGGTGTATGG-3′ (forward) and 5′-GAACGCCACGTAAAAGATGG-3′ (reverse); mANO1: 5′-GACGCCGAATGCAAGTATGGA-3′ (forward) and 5′- GTCCCCAGGACCATGTCATTT-3′ (reverse); hGAPDH: 5′-TCCCTGAGCTGAACGGGAAG-3′ (forward) and 5′-GGAGGAGTGGGTGTCGCTGT-3′ (reverse); and mGAPDH: 5′-TCACCACCATGGAGAAGGC-3′ (forward) and 5′-GCTAAGCAGTTGGTGGTGCA-3′ (reverse).

Capsaicin-induced pain-sensation and von Frey filament assays

Capsaicin-induced pain-sensation assays in mice were performed following a published protocol (19). Briefly, 10 μl of

capsaicin (300 μM) or solvent control was injected into the top of the hind paw by using a fine (30-G) needle; capsaicin was dissolved in 0.3% ethanol and 3% (v/v) dimethyl sulfoxide. The mice were wrapped gently in the investigator's hand and maintained on their back, with their snout pointing toward the small finger of the investigator; in this position, the mice remained unagitated during injection. Mouse behavior was recorded using a digital camera (GoPro5).

The von Frey filament assay was performed as per published procedures (63).

Saliva secretion assay

Saliva secretion was assayed as described (25). Briefly, 4- to 6-week-old mice were anesthetized, a small incision was made on the trachea to prevent choking, and pilocarpine hydrochloride (P6503; Sigma) was injected (at 10 mg/kg bodyweight) to induce chronic secretion of saliva. The saliva was collected for 20 min on a preweighed filter paper.

Miscellaneous methods

Cell-surface biotinylation assays, mouse tissue preparation for Western blotting, and heart-rate measurement were performed following our previously described protocols (21). The anesthetic used in the heart-rate measurement was 2.5% avertin in PBS plus 2.5% dimethyl sulfoxide (180 μl/20 g bodyweight).

Statistics

Protein bands in Western blots were quantified using ImageJ software. All data are expressed as the means ± SEM; n represents the number of independent biological replicates. Unless indicated otherwise, Student's two-tailed *t* test was used for statistical analysis, and $p < 0.05$ was considered statistically significant.

Data availability

All data presented are contained within the article.

Supporting information—This article contains supporting information (64).

Acknowledgments—We thank Drs Robert Tarran (University of North Carolina-Chapel Hill), Caroline Jefferies (Royal College of Surgeons in Ireland), and Kei-ichiro Arimoto (Moores UCSD Cancer Center) for kindly providing human ANO1 (originally from H. Criss Hartzell's laboratory), TRIM21, and TRIM23 cDNAs, respectively.

Author contributions—X. C., Z. Z., and P. H. conceptualization; X. C., Z. Z., Z. L., and R. H. methodology; X. C., Z. Z., and P. H. formal analysis; X. C., Z. Z., Y. T., Z. L., K. O. C., X. C., W. H., Y. M. W., and X. L. investigation; H. Z. and R. H. resources; X. C., Z. Z., and P. H. writing-original and draft; P. H. with contributions from all the authors writing-review and editing; X. C. and Z. Z. visualization; P. H. supervision; P. H. funding acquisition.

Funding and additional information—This work was supported by Hong Kong RGC GRF16102415, GRF16111616, GRF16102417, and GRF16100218, NSFC-RGC Joint Research Scheme N_HKUST614/18, Shenzhen Basic Research Scheme (JCYJ20170818114328332), and SMSEGL20SC01-K (all to P. H.). This work was supported in part by the Innovation and Technology Commission (ITCPD/17-9)

Conflict of interest—The authors declare that they have no conflicts of interest with the contents of this article.

Abbreviations—The abbreviations used are: ANO1, anoctamin-1; ANO1–V5, V5-tagged full-length ANO1; ANO1C, ANO1 C terminus; ARF, ADP-ribosylation factor; CHX, cycloheximide; co-IP, coimmunoprecipitation; CRISPR/Cas9, clustered regularly interspaced short palindromic repeat/CRISPR-associated protein 9; DRG, dorsal root ganglion; EGF, epidermal growth factor; FBS, fetal bovine serum; HA, hemagglutinin; HNSCC, head and neck squamous cell carcinoma; IMEM, Improved Minimum Essential Medium; IRF, interferon regulation factor; qPCR, quantitative PCR; RNAi, RNA interference; sgRNA, single-guide RNA; TRIM, tripartite motif.

References

1. Pedemonte, N., and Galietta, L. J. V. (2014) Structure and function of tmem16 proteins (anoctamins). *Physiol. Rev.* **94**, 419–459
2. Qu, Z., Yao, W., Yao, R., Liu, X., Yu, K., and Hartzell, C. (2014) The Ca(2+) -activated Cl(-) channel, ANO1 (TMEM16A), is a double-edged sword in cell proliferation and tumorigenesis. *Cancer Med.* **3**, 453–461
3. Dang, S., Feng, S., Tien, J., Peters, C. J., Bulkley, D., Lolicato, M., Zhao, J., Zuberbühler, K., Ye, W., Qi, L., Chen, T., Craik, C. S., Jan, Y. N., Minor, D. L., Cheng, Y., *et al.* (2017) Cryo-EM structures of the TMEM16A calciumactivated chloride channel. *Nature* **552**, 426–429
4. Caputo, A., Caci, E., Ferrera, L., Pedemonte, N., Barsanti, C., Sondo, E., Pfeffer, U., Ravazzolo, R., Zegarra-Moran, O., and Galietta, L. J. (2008) TMEM16A, a membrane protein associated with calcium-dependent chloride channel activity. *Science* **322**, 590–594
5. Mroz, M. S., and Keely, S. J. (2012) Epidermal growth factor chronically upregulates Ca 2+-dependent Cl - conductance and TMEM16A expression in intestinal epithelial cells. *J. Physiol.* **590**, 1907–1920
6. Britschgi, A., Bill, A., Brinkhaus, H., Rothwell, C., Clay, I., Duss, S., Rebhan, M., Raman, P., Guy, C. T., Wetzel, K., George, E., Popa, M. O., Lilley, S., Choudhury, H., Gosling, M., *et al.* (2013) Calcium-activated chloride channel ANO1 promotes breast cancer progression by activating EGFR and CAMK signaling. *Proc. Natl. Acad. Sci. U. S. A.* **110**, E1026–E1034
7. Duran, C., and Hartzell, H. C. (2011) Physiological roles and diseases of tmem16/anoctamin proteins: Are they all chloride channels? *Acta Pharmacol. Sin.* **32**, 685–692
8. Duvvuri, U., Shiwarski, D. J., Xiao, D., Bertrand, C., Huang, X., Edinger, R. S., Rock, J. R., Harfe, B. D., Henson, B. J., Kunzelmann, K., Schreiber, R., Seethala, R. S., Egloff, A. M., Chen, X., Lui, V. W., *et al.* (2012) TMEM16A induces MAPK and contributes directly to tumorigenesis and cancer progression. *Cancer Res.* **72**, 3270–3281
9. Liu, W., Lu, M., Liu, B., Huang, Y., and Wang, K. W. (2012) Inhibition of Ca2+-activated Cl- channel ANO1/TMEM16A expression suppresses tumor growth and invasiveness in human prostate carcinoma. *Cancer Lett.* **326**, 41–51
10. Zhang, C. H., Li, Y., Zhao, W., Lifshitz, L. M., Li, H., Harfe, B. D., Zhu, M. S., and ZhuGe, R. (2013) The transmembrane protein 16A Ca2+-activated Cl channel in airway smooth muscle contributes to airway hyperresponsiveness. *Am. J. Respir. Crit. Care Med.* **187**, 374–381
11. Wang, M., Yang, H., Zheng, L. Y., Zhang, Z., Tang, Y. B., Wang, G. L., Du, Y. H., Lv, X. F., Liu, J., Zhou, J. G., and Guan, Y. Y. (2012) Downregulation of TMEM16A calcium-activated chloride channel contributes

to cerebrovascular remodeling during hypertension by promoting basilar smooth muscle cell proliferation. *Circulation* **125**, 697–707
12. Scudieri, P., Caci, E., Bruno, S., Ferrera, L., Schiavon, M., Sondo, E., Tomati, V., Gianotti, A., Zegarra-Moran, O., Pedemonte, N., Rea, F., Ravazzolo, R., and Galietta, L. J. V. (2012) Association of TMEM16A chloride channel overexpression with airway goblet cell metaplasia. *J. Physiol.* **590**, 6141–6155
13. Ozato, K., Shin, D. M., Chang, T. H., and Morse, H. C. (2008) TRIM family proteins and their emerging roles in innate immunity. *Nat. Rev. Immunol.* **8**, 849–860
14. Reymond, A., Meroni, G., Fantozzi, A., Merla, G., Cairo, S., Luzi, L., Riganelli, D., Zanaria, E., Messali, S., Cainarca, S., Guffanti, A., Minucci, S., Pelicci, P. G., and Ballabio, A. (2001) The tripartite motif family identifies cell compartments. *EMBO J.* **20**, 2140–2151
15. Vichi, A., Payne, D. M., Pacheco-Rodriguez, G., Moss, J., and Vaughan, M. (2005) E3 ubiquitin ligase activity of the trifunctional ARD1 (ADP-ribosylation factor domain protein 1). *Proc. Natl. Acad. Sci. U. S. A.* **102**, 1945–1950
16. Liu, Z., Chen, P., Gao, H., Gu, Y., Yang, J., Peng, H., Xu, X., Wang, H., Yang, M., Liu, X., Fan, L., Chen, S., Zhou, J., Sun, Y., Ruan, K., *et al.* (2014) Ubiquitylation of autophagy receptor optineurin by HACE1 activates selective autophagy for tumor suppression. *Cancer Cell* **26**, 106–120
17. Meza-Carmen, V., Pacheco-Rodriguez, G., Kang, G. S., Kato, J., Donati, C., Zhang, C. Y., Vichi, A., Payne, D. M., El-Chemaly, S., Stylianou, M., Moss, J., and Vaughan, M. (2011) Regulation of growth factor receptor degradation by ADP-ribosylation factor domain protein (ARD) 1. *Proc. Natl. Acad. Sci. U. S. A.* **108**, 10454–10459
18. Hirano, A., Yumimoto, K., Tsunematsu, R., Matsumoto, M., Oyama, M., Kozuka-Hata, H., Nakagawa, T., Lanjakornsiripan, D., Nakayama, K. I., and Fukada, Y. (2013) FBXL21 regulates oscillation of the circadian clock through ubiquitination and stabilization of cryptochromes. *Cell* **152**, 1106–1118
19. Takayama, Y., Uta, D., Furue, H., and Tominaga, M. (2015) Pain-enhancing mechanism through interaction between TRPV1 and anoctamin 1 in sensory neurons. *Proc. Natl. Acad. Sci. U. S. A.* **112**, 5213–5218
20. Liu, B., Linley, J. E., Du, X., Zhang, X., Ooi, L., Zhang, H., and Gamper, N. (2010) The acute nociceptive signals induced by bradykinin in rat sensory neurons are mediated by inhibition of M-type K+ channels and activation of Ca2+-activated Cl- channels. *J. Clin. Invest.* **120**, 1240–1252
21. Hu, W., Yu, X., Liu, Z., Sun, Y., Chen, X., Yang, X., Li, X., Lam, W. K., Duan, Y., Cao, X., Steller, H., Liu, K., and Huang, P. (2017) The complex of TRIP-Br1 and XIAP ubiquitinates and degrades multiple adenylyl cyclase isoforms. *Elife* **6**, e28021
22. Cheng, Y. F., Chang, Y. T., Chen, W. H., Shih, H. C., Chen, Y. H., Shyu, B. C., and Chen, C. C. (2017) Cardioprotection induced in a mouse model of neuropathic pain via anterior nucleus of paraventricular thalamus. *Nat. Commun.* **8**, 826
23. D'souza, A., Bucchi, A., Johnsen, A. B., Logantha, S. J. R. J., Monfredi, O., Yanni, J., Prehar, S., Hart, G., Cartwright, E., Wisloff, U., Dobryznski, H., Difrancesco, D., Morris, G. M., and Boyett, M. R. (2014) Exercise training reduces resting heart rate via downregulation of the funny channel HCN4. *Nat. Commun.* **5**, 3775
24. Catalan, M. A., Kondo, Y., Pena-Munzenmayer, G., Jaramillo, Y., Liu, F., Choi, S., Crandall, E., Borok, Z., Flodby, P., Shull, G. E., and Melvin, J. E. (2015) A fluid secretion pathway unmasked by acinar-specific Tmem16A gene ablation in the adult mouse salivary gland. *Proc. Natl. Acad. Sci. U. S. A.* **112**, 2263–2268
25. Gautam, D., Heard, T. S., Cui, Y., Miller, G., Bloodworth, L., and Wess, J. (2004) Cholinergic stimulation of salivary secretion studied with M1 and M3 muscarinic receptor single- and double-knockout mice. *Mol. Pharmacol.* **66**, 260–267
26. Perez-Cornejo, P., Gokhale, A., Duran, C., Cui, Y., Xiao, Q., Hartzell, H. C., and Faundez, V. (2012) Anoctamin 1 (Tmem16A) Ca2+-activated chloride channel stoichiometrically interacts with an ezrin-radixin-moesin network. *Proc. Natl. Acad. Sci. U. S. A.* **109**, 10376–10381
27. Yoo, S. H., Mohawk, J. A., Siepka, S. M., Shan, Y., Huh, S. K., Hong, H. K., Kornblum, I., Kumar, V., Koike, N., Xu, M., Nussbaum, J., Liu, X., Chen, Z., Chen, Z. J., Green, C. B., *et al.* (2013) Competing E3 ubiquitin ligases govern circadian periodicity by degradation of CRY in nucleus and cytoplasm. *Cell* **152**, 1091–1105
28. Ozato, K., Yoshimi, R., Chang, T.-H., Wang, H., Atsumi, T., and Morse, H. C. (2009) Comment on "gene disruption study reveals a nonredundant role for TRIM21/Ro52 in NF-κB-dependent cytokine expression in fibroblasts": Figure 1. *J. Immunol.* **183**, 7619
29. Nakamura, T., Matsui, M., Uchida, K., Futatsugi, A., Kusakawa, S., Matsumoto, N., Nakamura, K., Manabe, T., Taketo, M. M., and Mikoshiba, K. (2004) M3 muscarinic acetylcholine receptor plays a critical role in parasympathetic control of salivation in mice. *J. Physiol.* **558**, 561–575
30. Bill, A., Gutierrez, A., Kulkarni, S., Kemp, C., Bonenfant, D., Voshol, H., Duvvuri, U., and Alex Gaither, L. (2015) ANO1/TMEM16A interacts with EGFR and correlates with sensitivity to EGFR-targeting therapy in head and neck cancer. *Oncotarget* **6**, 9173–9188
31. Watanabe, M., Takahashi, H., Saeki, Y., Ozaki, T., Itoh, S., Suzuki, M., Mizushima, W., Tanaka, K., and Hatakeyama, S. (2015) The E3 ubiquitin ligase TRIM23 regulates adipocyte differentiation via stabilization of the adipogenic activator PPARgamma. *Elife* **4**, e05615
32. Arimoto, K. I., Funami, K., Saeki, Y., Tanaka, K., Okawa, K., Takeuchi, O., Akira, S., Murakami, Y., and Shimotohno, K. (2010) Polyubiquitin conjugation to NEMO by triparite motif protein 23 (TRIM23) is critical in antiviral defense. *Proc. Natl. Acad. Sci. U. S. A.* **107**, 15856–15861
33. Laurent-Rolle, M., Morrison, J., Rajsbaum, R., Macleod, J. M. L., Pisanelli, G., Pham, A., Ayllon, J., Miorin, L., Martínez-Romero, C., Tenoever, B. R., and García-Sastre, A. (2014) The interferon signaling antagonist function of yellow fever virus NS5 protein is activated by type i interferon. *Cell Host Microbe* **16**, 314–327
34. Chen, Z. J., and Sun, L. J. (2009) Nonproteolytic functions of ubiquitin in cell signaling. *Mol. Cell* **33**, 275–286
35. Jin, X., Jin, H. R., Jung, H. S., Lee, S. J., Lee, J. H., and Lee, J. J. (2010) An atypical E3 ligase zinc finger protein 91 stabilizes and activates NF-kappaB-inducing kinase via Lys63-linked ubiquitination. *J. Biol. Chem.* **285**, 30539–30547
36. Zeng, S., Wang, Y., Zhang, T., Bai, L., Wang, Y., and Duan, C. (2017) E3 ligase UHRF2 stabilizes the acetyltransferase TIP60 and regulates H3K9ac and H3K14ac via RING finger domain. *Protein Cell* **8**, 202–218
37. Yang, L., Jin, L., Ke, Y., Fan, X., Zhang, T., Zhang, C., Bian, H., and Wang, G. (2018) E3 ligase Trim21 ubiquitylates and stabilizes keratin 17 to induce STAT3 activation in psoriasis. *J. Invest. Dermatol.* **138**, 2568–2577
38. Xu, S. H., Zhu, S., Wang, Y., Huang, J. Z., Chen, M., Wu, Q. X., He, Y. T., Chen, and Yan, G. R. (2018) ECD promotes gastric cancer metastasis by blocking E3 ligase ZFP91-mediated hnRNP F ubiquitination and degradation. *Cell Death Dis.* **9**, 479
39. Pan, J. A., Sun, Y., Jiang, Y. P., Bott, A. J., Jaber, N., Dou, Z., Yang, B., Chen, J. S., Catanzaro, J. M., Du, C., Ding, W. X., Diaz-Meco, M. T., Moscat, J., Ozato, K., Lin, R. Z., *et al.* (2016) TRIM21 ubiquitylates SQSTM1/p62 and suppresses protein sequestration to regulate redox homeostasis. *Mol. Cell* **62**, 149–151
40. Xue, B., Li, H., Guo, M., Wang, J., Xu, Y., Zou, X., Deng, R., Li, G., and Zhu, H. (2018) TRIM21 promotes innate immune response to RNA viral infection through Lys27-linked polyubiquitination of MAVS. *J. Virol.* **92**, e00321-18
41. Espinosa, A., Dardalhon, V., Brauner, S., Ambrosi, A., Higgs, R., Quintana, F. J., Sjostrand, M., Eloranta, M. L., Ni Gabhann, J., Winqvist, O., Sundelin, B., Jefferies, C. A., Rozell, B., Kuchroo, V. K., and Wahren-Herlenius, M. (2009) Loss of the lupus autoantigen Ro52/Trim21 induces tissue inflammation and systemic autoimmunity by disregulating the IL-23-Th17 pathway. *J. Exp. Med.* **206**, 1661–1671
42. Itou, J., Li, W., Ito, S., Tanaka, S., Matsumoto, Y., Sato, F., and Toi, M. (2018) Sal-like 4 protein levels in breast cancer cells are post-translationally down-regulated by tripartite motif-containing 21. *J. Biol. Chem.* **293**, 6556–6564
43. Lazzari, E., Korczeniewska, J., Ni Gabhann, J., Smith, S., Barnes, B. J., and Jefferies, C. A. (2014) TRIpartite motif 21 (TRIM21) differentially regulates the stability of interferon regulatory factor 5 (IRF5) isoforms. *PLoS One* **9**, e103609
44. Wei, Z., Song, J., Wang, G., Cui, X., Zheng, J., Tang, Y., Chen, X., Li, J., Cui, L., Liu, C. Y., and Yu, W. (2018) Deacetylation of serine

hydroxymethyl-transferase 2 by SIRT3 promotes colorectal carcinogenesis. *Nat. Commun.* **9**, 4468
45. Duan, D. D. (2013) Phenomics of cardiac chloride channels. *Compr. Physiol.* **3**, 667–692
46. Ye, Z., Wu, M. M., Wang, C. Y., Li, Y. C., Yu, C. J., Gong, Y. F., Zhang, J., Wang, Q. S., Song, B. L., Yu, K., Hartzell, H. C., Duan, D. D., Zhao, D., and Zhang, Z. R. (2015) Characterization of cardiac anoctamin1 Ca2+-activated chloride channels and functional role in ischemia-induced arrhythmias. *J. Cell Physiol.* **230**, 337–346
47. Migliaccio, A., Di Domenico, M., Castoria, G., Nanayakkara, M., Lombardi, M., De Falco, A., Bilancio, A., Varricchio, L., Ciociola, A., and Auricchio, F. (2005) Steroid receptor regulation of epidermal growth factor signaling through Src in breast and prostate cancer cells: Steroid antagonist action. *Cancer Res.* **65**, 10585–10593
48. González, L., Díaz, M. E., Miquet, J. G., Sotelo, A. I., Fernández, D., Dominici, F. P., Bartke, A., and Turyn, D. (2010) GH modulates hepatic epidermal growth factor signaling in the mouse. *J. Endocrinol.* **204**, 299–309
49. González, E. A., Disthabanchong, S., Kowalewski, R., and Martin, K. J. (2002) Mechanisms of the regulation of EGF receptor gene expression by calcitriol and parathyroid hormone in UMR 106-01 cells. *Kidney Int.* **61**, 1627–1634
50. Dickson, C., Fletcher, A. J., Vaysburd, M., Yang, J.-C., Mallery, D. L., Zeng, J., Johnson, C. M., McLaughlin, S. H., Skehel, M., Maslen, S., Cruickshank, J., Huguenin-Dezot, N., Chin, J. W., Neuhaus, D., and James, L. C. (2018) Intracellular antibody signalling is regulated by phosphorylation of the Fc receptor TRIM21. *Elife* **7**, e32660
51. Sjostrand, M., Ambrosi, A., Brauner, S., Sullivan, J., Malin, S., Kuchroo, V. K., Espinosa, A., and Wahren-Herlenius, M. (2013) Expression of the immune regulator tripartite-motif 21 is controlled by IFN regulatory factors. *J. Immunol.* **191**, 3753–3763
52. Wang, H., Zou, L., Ma, K., Yu, J., Wu, H., Wei, M., and Xiao, Q. (2017) Cell-specific mechanisms of TMEM16A Ca(2+)-activated chloride channel in cancer. *Mol. Cancer* **16**, 152
53. Cha, J. Y., Wee, J., Jung, J., Jang, Y., Lee, B., Hong, G. S., Chang, B. C., Choi, Y. L., Shin, Y. K., Min, H. Y., Lee, H. Y., Na, T. Y., Lee, M. O., and Oh, U. (2015) Anoctamin 1 (TMEM16A) is essential for testosterone-induced prostate hyperplasia. *Proc. Natl. Acad. Sci. U. S. A.* **112**, 9722–9727
54. Zhou, W., Zhang, Y., Zhong, C., Hu, J., Hu, H., Zhou, D., and Cao, M. (2018) Decreased expression of TRIM21 indicates unfavorable outcome and promotes cell growth in breast cancer. *Cancer Manag. Res.* **10**, 3687–3696
55. Yao, Y., Liu, Z., Guo, H., Huang, S., Zhong, M., Deng, J., and Xiong, J. (2018) Elevated TRIM23 expression predicts poor prognosis in Chinese gastric cancer. *Pathol. Res. Pract.* **214**, 2062–2068
56. Valach, J., Fik, Z., Strnad, H., Chovanec, M., Plzak, J., Cada, Z., Szabo, P., Sachova, J., Hroudova, M., Urbanova, M., Steffl, M., Paces, J., Mazanek, J., Vlcek, C., Betka, J., *et al.* (2012) Smooth muscle actin-expressing stromal fibroblasts in head and neck squamous cell carcinoma: Increased expression of galectin-1 and induction of poor prognosis factors. *Int. J. Cancer* **131**, 2499–2508
57. Rotin, D., and Staub, O. (2011) Role of the ubiquitin system in regulating ion transport. *Pflugers Arch. Eur. J. Physiol.* **461**, 1–21
58. Yoshimi, R., Chang, T. H., Wang, H., Atsumi, T., Morse, H. C., 3rd, and Ozato, K. (2009) Gene disruption study reveals a nonredundant role for TRIM21/Ro52 in NF-kappaB-dependent cytokine expression in fibroblasts. *J. Immunol.* **182**, 7527–7538
59. Wang, H., Yang, H., Shivalila, C. S., Dawlaty, M. M., Cheng, A. W., Zhang, F., and Jaenisch, R. (2013) One-step generation of mice carrying mutations in multiple genes by CRISPR/Cas-mediated genome engineering. *Cell* **153**, 910–918
60. Ran, F. A., Hsu, P. D., Wright, J., Agarwala, V., Scott, D. A., and Zhang, F. (2013) Genome engineering using the CRISPR-Cas9 system. *Nat. Protoc.* **8**, 2281–2308
61. Duan, Y., Sun, Y., Zhang, F., Zhang, W. K., Wang, D., Wang, Y., Cao, X., Hu, W., Xie, C., Cuppoletti, J., Magin, T. M., Wang, H., Wu, Z., Li, N., and Huang, P. (2012) Keratin K18 increases cystic fibrosis transmembrane conductance regulator (CFTR) surface expression by binding to its C-terminal hydrophobic patch. *J. Biol. Chem.* **287**, 40547–40559
62. Sun, Y., Duan, Y., Eisenstein, A. S., Hu, W., Quintana, A., Lam, W. K., Wang, Y., Wu, Z., Ravid, K., and Huang, P. (2012) A novel mechanism of control of NFkappaB activation and inflammation involving A2B adenosine receptors. *J. Cell Sci.* **125**, 4507–4517
63. Lee, B., Cho, H., Jung, J., Yang, Y. D., Yang, D. J., and Oh, U. (2014) Anoctamin 1 contributes to inflammatory and nerve-injury induced hypersensitivity. *Mol. Pain* **10**, 5
64. Yu, X., Zhao, Q., Li, X., Chen, Y., Tian, Y., Liu, S., Xiong, W., and Huang, P. (2020) Deafness mutation D572N of TMC1 destabilizes TMC1 expression by disrupting LHFPL5 binding. *Proc. Natl. Acad. Sci. U. S. A.* **117**, 29894–29903

Xu Cao received his PhD from the Hong Kong University of Science and Technology. Now, he is an engineer in Genvida (HK), an interdisciplinary startup company that is developing solid-state nanopore sequencing, the fourth-generation sequencing technique. His research interest focuses on the chemical and physical regulation of ion channels, either native ANO1 and CFTR channel or artificially fabricated nanopores.

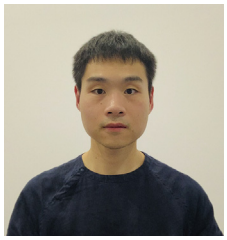

Zijing Zhou received his PhD from the Hong Kong University of Science and Technology and is now working at the Victor Chang Cardiac Research Institute, Australia. His research is focused on understanding the post-translational modifications and trafficking pathways of ion channels, especially the mechanosensitive channels, under normal or pathological conditions. He is combing biochemical and biophysical approaches to elucidate the mechanisms regulating the maturation of such channels. More of him can be found with the link: https://www.researchgate.net/profile/Zijing-Zhou-3.